CHAPTER 4

Well Log Analysis and Seismic Interpretation

4.1 Introduction

Seismic and well log data sets are combined to illustrate structural and reservoir characterization analysis. This chapter is divided into 3 major parts which are well log interpretation and analysis, well to seismic tie and seismic interpretation. Figure 4.1 shows the base map of the 3D seismic survey and location of the Well A, Inlines (from 1240 to 2000) in red color are North West - South East direction while crosslines (from 4420 to 5270) in blue color are South West - North East direction.

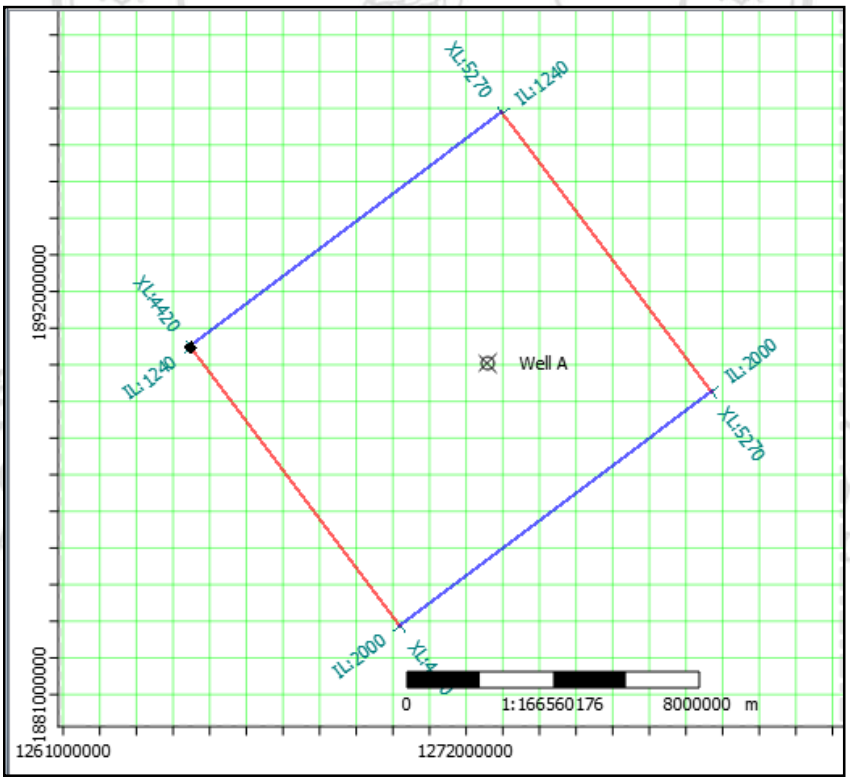

Figure 4.1: Base map of the study area. Inlines are represented by red color while crosslines are represented by blue color.

Hampson Russell software packages (HRS-9) were used for log editing and calculation, application for fluid substitution, check shot calibration and plot the data. Interactive Petrophysics (IP 3.5) was used for well logs interpretation. Petrel 2013 software has been used for generating seismic attribute volumes. Kingdom Suite 8.8 software was used for 3D seismic interpretation, structural and seismic attributes mapping.

4.2 Well Log Analysis and Interpretation

Well logs data provide important information to define reservoirs and other important intervals throughout the well. In this study, Well A has sufficient logs with good quality. Four reservoir intervals name UMA15, MMF10, MMF15 and MMF30 limited by tops and bases that is provided by the company. Because two main reservoir intervals in the Well A is UMA15 from 2999.1 m to 3014.4 m (MD) and MMF30 from 3583 m to 3616 m (MD), well logs interpretation is mainly around zone of interest from 2900 m to 3700 m (MD). Figure 4.2 shows the available logs from Well A using mainly in Hampson Russell software, the whole well logs data in this study is shown in Table 3.1. The rest of logs like LLS and MSFL are used in Interactive Petrophysics software for interpretation.

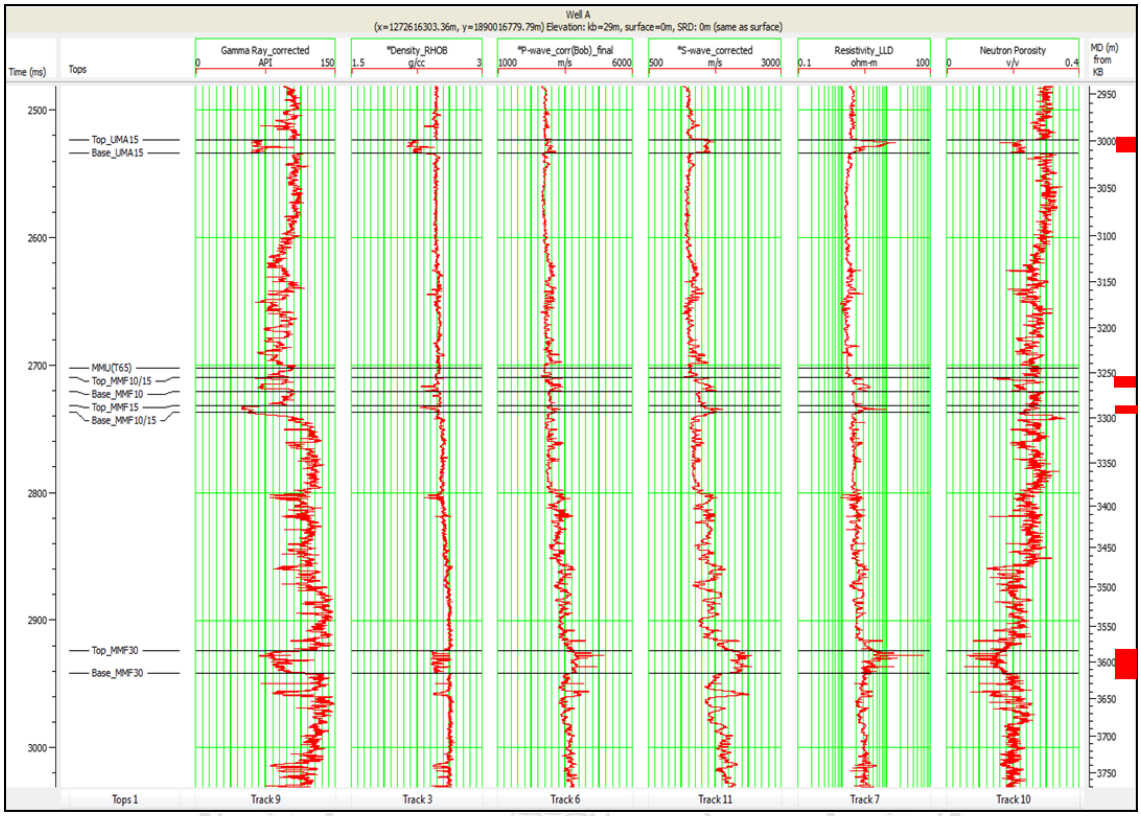

Figure 4.2: Available logs from Well A (from left to right: GR, Density, P-wave velocity, S-wave velocity, Resistivity, Neutron porosity). The red squares indicate potential reservoir intervals.

4.2.1 Gamma Ray Log

Gamma ray log (GR) measures the natural radioactivity in formations in the well (naturally accruing or put there in mud system) which connected to clay mineral, oil source rock, organic matter and shale in the reservoir (Schlumberger, 1972). Gamma ray log is known normally as the most reliable in identifying lithology and correlating zones with different petrophysical properties. Conventional reservoir rocks like shale-free sandstones and carbonates have low concentrations with the radioactive material, therefore it shows low gamma ray values. In contrast, as the shale content increases, the gamma ray log show increase in values due to the high concentrations with radioactive material of shale.

As shown in Figure 4.2, it is clearly that there are transitions between shale units and sand units. UMA15 interval, from 2999.1 m to 3014.4 m, shows GR values around 50 API to 64 API. MMF10 interval, from 3254.6 m to 3270.9 m, shows GR values around

65 API to 75 API, however in this interval there is a thin shale (high GR values) interval from 3257 m to 3262 m which separated MMF10 to upper and lower sand interval. MMF15 interval, from 3287 m to 3294.6 m, shows GR values around 49 API to 60 API. MMF30 interval, from 3583 m to 3616 m, shows GR values around 55 API to 65 API. The thin lower sandstone interval from 3638 m to 3647 m, shows GR values around 86 API to 120 API. However, it is mentioned that not to contain movable hydrocarbons in the final well report. The rapid decrease in gamma ray log typically shows that log moves to low content of shale intervals that are sandstone formations.

4.2.2 Density Log

Density log measures the electron density of the formation (number of electrons per unit volume). The electron density can be related to the actual density of the formation. Density log primarily is used as porosity logs. Other main uses of it including identification of minerals in evaporate deposits, detection of gas-bearing zones, determination hydrocarbon density and evaluation shaly-sand reservoirs and complex lithology (Schlumberger, 1972). In general, the density of shale units is higher than sand units.

As shown in Figure 4.2, the Well A's density log shows low density of around 2.13 g/cc to 2.32 g/cc in the UMA15 reservoir at 2999.1 - 3014.4 m. For the MMF10 reservoir, the density log shows almost no low density values while the MMF15 reservoir's the density log shows just around 2.26 g/cc to 2.70 g/cc at 3287 – 3290 m. For the MMF30 reservoir, the density log shows low density of around 2.4 g/cc to 2.6 g/cc at 3583 – 3616 m. Not all sand units in Well A show low densities, but two main reservoir interval UMA15 and MMF30 show low densities in whole sand interval. It is clearly that density log from Well A strongly affected by the presence of gas in sand bodies UMA15 and MMF30.

4.2.3 P-wave Velocity

The sonic tools measure the velocity of sound in the formation. The log is scaled in slowness which is the reciprocal of velocity. A P-wave sonic log measures interval transit time of a compressional wave travelling through the formation (Asquith,G. et al.,2004). The main applications of the sonic log are seismic time to depth conversion,

synthetic seismograms (combination with the density log), mechanical properties of rocks (combination with the density log) and porosity.

Hydrocarbon effects cause the increasing in interval transit time of a formation. In Well A, as shown in Figure 4.2, the P-wave velocity log shows slight increase in UMA15 of around 10 % and a high increase in MMF30 of around 15%. This is because of hydrocarbon presence in the formation especially for the MMF30 reservoir interval.

4.2.4 S-wave Velocity

It is obvious that S-wave velocity data will be useful in calculating rock elastic or inelastic properties and as an adjunct to shear seismic data. S-wave transit time is also useful in identifying matrix minerals and pore fluids and fluid identification (Schlumberger, 1972). S-wave velocity is always slower than P-wave velocity for the same formation. In Well A, the S-wave sonic log is recorded from 2897.28 m to 4144.62 m, this cover all the interest intervals. It shows good quality that has been proved by editing and cross plots with P-wave velocity in chapter 3. As shown in Figure 4.2, the S-wave velocity has as same tendency as the P-wave velocity in the velocity increase at the reservoir intervals. The S-wave velocity also shows high increase in UMA15, MMF10 and MMF15 of around 15 % and a high increase in MMF30 of around 25 %. This is because of hydrocarbon presence in the formation especially for the MMF30 reservoir interval.

Figure 4.3 shows cross plot of P-wave velocity versus S-wave velocity at interval from 2897.27 m to 3750 m which covers all reservoirs. Color of data is sorted by gamma ray log. There are two different trends, the trend line through the red rectangular zone shows gas bearing sandstone area meanwhile the rest trend line shows non-reservoir area (water saturated sand and shaly sand) and shale. Variations in porosity, shaliness, and pore pressure move data up and down along the trends, while changes in fluid saturation move data from one to another (Per Avseth et al., 2005).

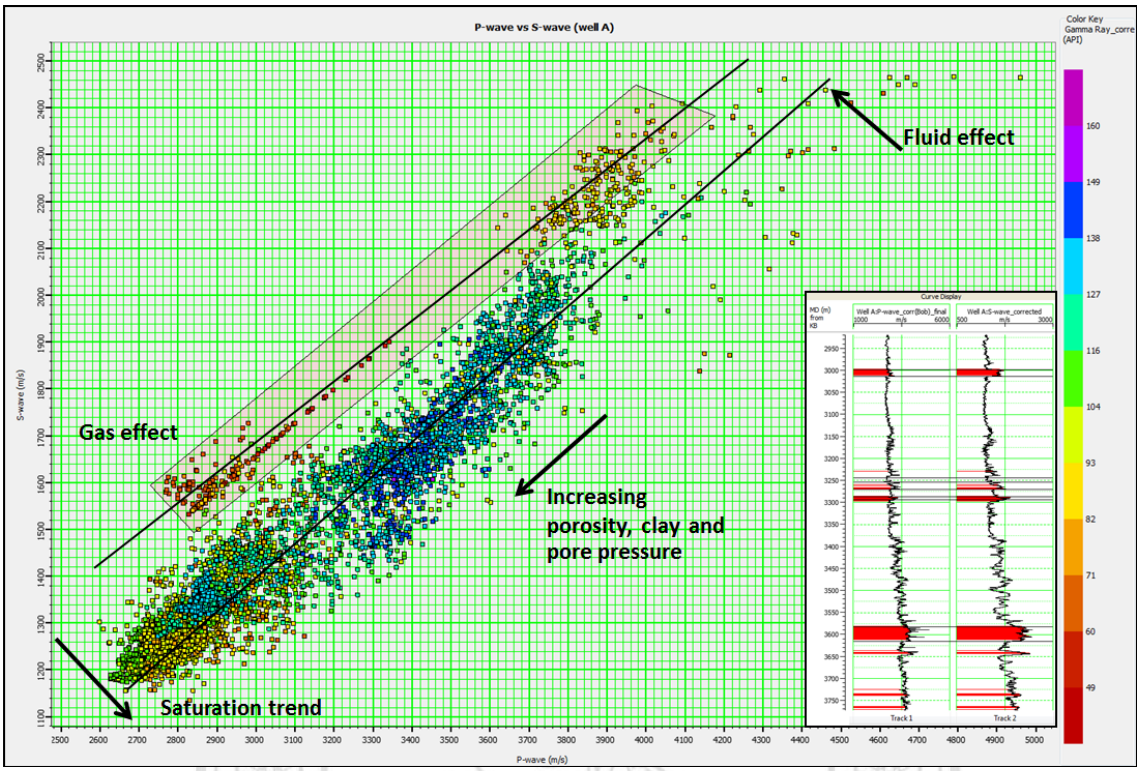

Figure 4.3: Cross plot of Vp and Vs of Well A from 2897.27 m to 3750 m. The black arrow indicates the increasing of porosity, clay and pore pressure perpendicular with the saturation trend. The red rectangular represents the gas effect in the reservoir intervals.

4.2.5 Neutron Porosity Log

Neutron logs are porosity logs that measure the hydrogen concentration in the formations (Schlumberger, 1972). In clean formations where the porosity is filled with water or oil, the neutron log measures liquid-filled porosity. Not as density log is lithology independent, the neutron porosity log is always displayed as porosity, so it is lithology dependent and it is very important to know which lithology is used to display porosity in the reservoirs. In Well A, the neutron log is displayed in sandstone units. The neutron porosity log shows low values in reservoir intervals, this means less hydrogen atoms and there is presence of gas in the sand layers.

Gas zones can often be identified by comparing the neutron log with another porosity log, Figure 4.4 shows the plot of the neutron log with the density log. It is clearly that there are two overlaps intervals in UMA15 reservoir and MMF30 reservoir. This indicates gas bearing zone in UMA15 and MMF30. Besides, in MMF10 and MMF15 reservoir interval, there is just small overlap zones between the neutron log and the

density log. This may indicates there is little hydrocarbon in these zones. The neutron log shows value of 0.23 to 0.17 and 0.06 to 0.15 at UMA15 interval and MMF30 interval respectively. Therefore, these two reservoirs intervals would be main reservoirs in the Well A.

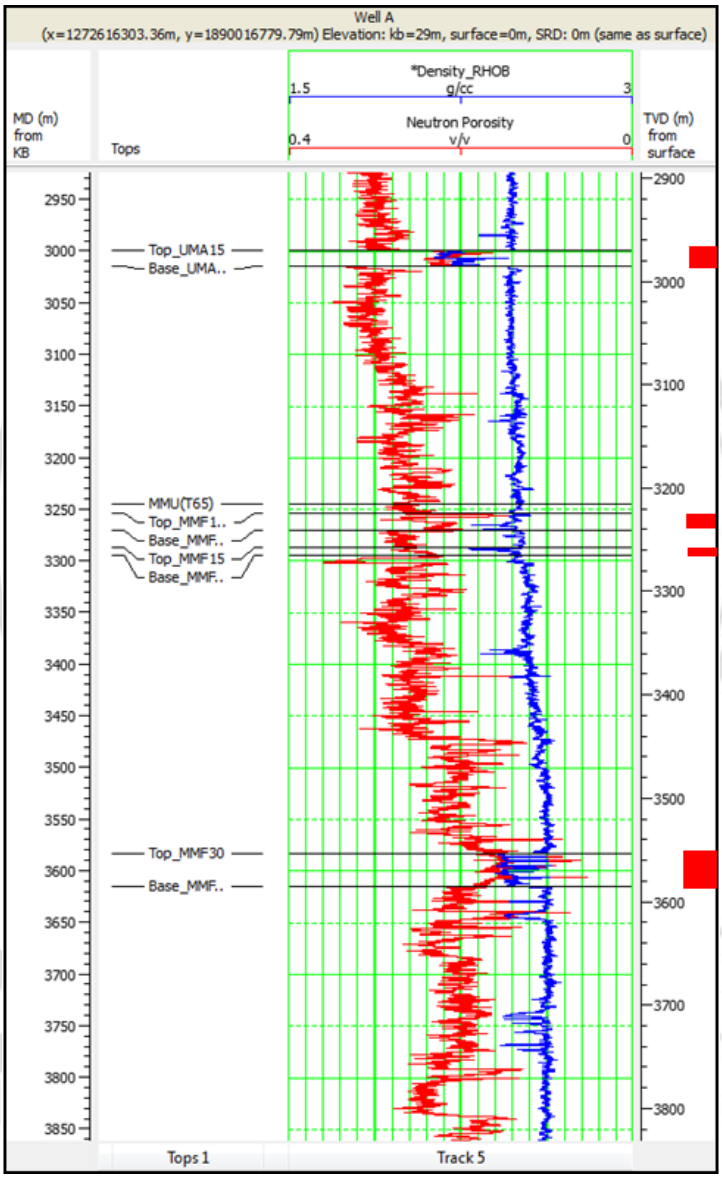

Figure 4.4: Plot between the Density Log in blue and the Neutron Porosity Log in red color in the interest zone.

4.2.6 Resistivity Log

Resistivity logs are used mainly to determine hydrocarbon-bearing versus water-bearing zones indicate permeable zones and determine porosity (Asquith,G. et al.,2004). However, the most important use of resistivity logs is the determination of hydrocarbon-

bearing versus water-bearing zones due to the main physical property to differentiate water and hydrocarbons based on resistivity. Good conductors have very low resistivity, high conductivity such as salty water, metals copper, gold, etc. Meanwhile good insulators have very high resistivity and very low conductivity such as oil and gas, dry rock, plastic, dry wood etc. Therefore it expects low resistivity values in brine saturated rock and high resistivity values in hydrocarbon saturated rock.

Combination of Gamma Ray log and Resistivity log is typically used to differentiate hydrocarbon and non-hydrocarbon zone. As shown in Figure 4.2, throughout the depth of Well A, the Resistivity log shows high values in four zones. For UMA15 (GR values ~ 60 - 70 API), the resistivity log shows values of around 1.9 Ohmm to 12.6 Ohmm at 2999.1 - 3014.4 m. For MMF30 (GR values ~ 70 – 100 API), resistivity log shows values of around 3.6 Ohmm to 33 Ohmm at 3583 – 3616 m. Other zones show resistivity values fluctuating from lowest around 1 Ohmm to the highest 7 Ohmm. It is clearly that there is a significant different in resistivity values from gas-bearing sandstone units that shale dominated units.

4.3 Generate Other Logs and Interpretations

4.3.1 Vp/Vs Ratio

The velocity ratio (Vp/Vs ratio) has been used for many purposes such as lithology indicator, determining degree of consolidation, identifying pore fluid and predicting velocities (Myung W.Lee, 2003). Many rock physic researches and case studies suggested that the Vp/Vs ratio depends mainly on porosity, clay content, pore pressure and geometry and other factors. The P-wave can propagate through fluids and it is more sensitive with fluids. It shows high values responses when go through gas-bearing area. In contrast, the S-wave cannot propagate through fluids so it is not sensitive with fluids. Combination of the P-wave velocity, the S-wave velocity and Vp/Vs ratio helps separating lithology, pore pressure and saturation.

Figure 4.5 shows cross plot between Vp/Vs and Vs of Well A from 2897.27 m to 3750 m. Color of data is sorted by Gamma Ray log. It shows good separation of gas saturated rocks (in red oval zone) with water saturated rock and shale when the velocities are low and poor separation when the velocities are high which means rocks are deeper and

more consolidated. The trend in pore pressure is perpendicular with saturation trend. Figure 4.6 shows the cross section for Vp/Vs and Vs cross plot, the red colors in the logs represent red oval zone in cross plot.

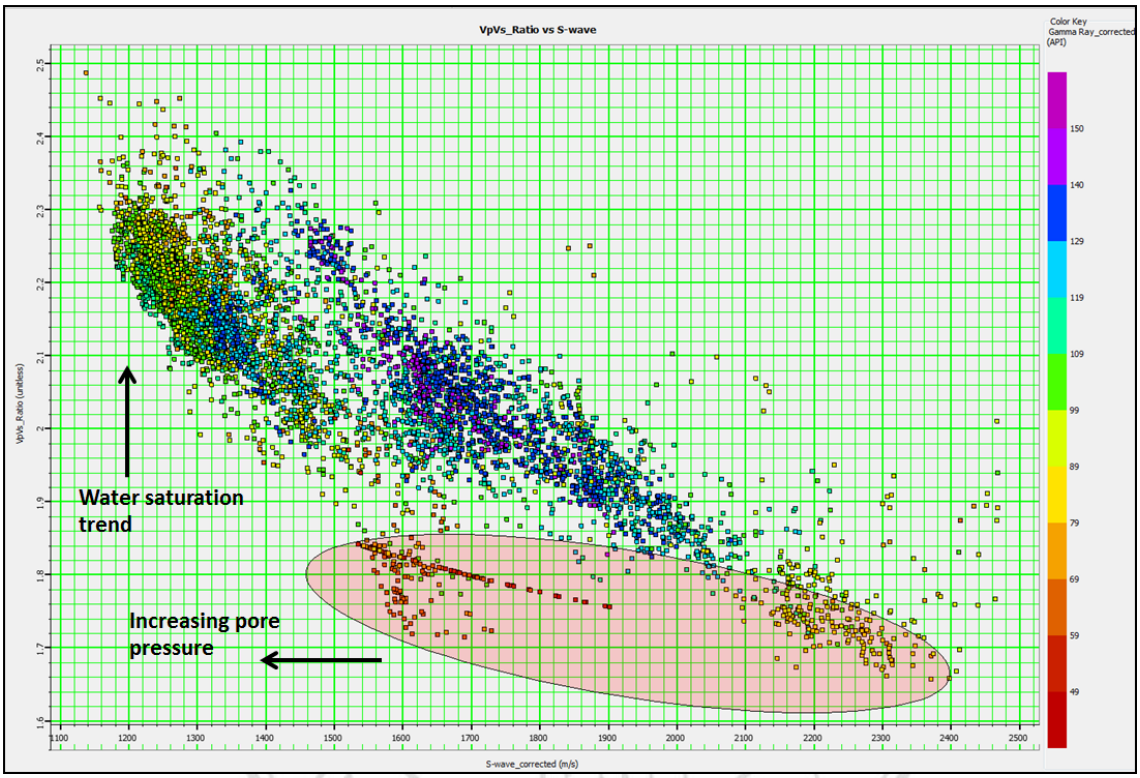

Figure 4.5: Cross plot of Vp/Vs ratio and S-wave velocity of Well A. The red oval zone represents reservoir intervals.

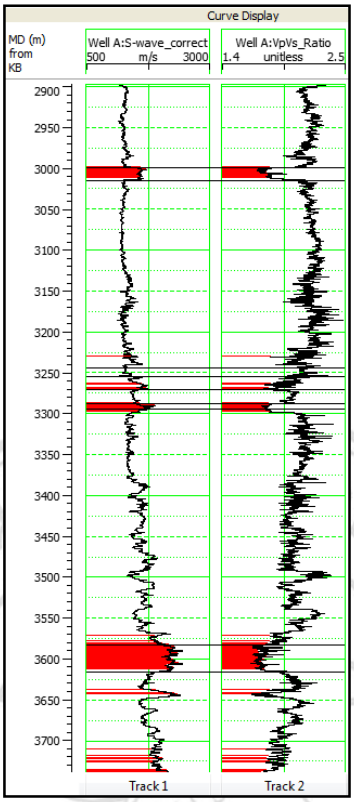

Figure 4.6: Cross section for Vp/Vs and S-wave velocity cross plot.

4.3.2 Poisson's Ratio

Poisson's ratio is an important elastic parameter in AVO and inversion analysis. It is the ratio of fractional change in width to the fractional change in length under uni-axial compression (Simm & Bacon, 2014). It can be shown as equation:

$$Poisson\ ratio\ (\sigma) = -\frac{Transverse\ strain}{Longitudinal\ strain} = \frac{3K-2\mu}{2(3K+\mu)}, \quad (4.1)$$

where K is bulk modulus and μ is shear modulus. It is almost always in positive value. Poisson's ratio can be derived using many ways such as velocity method using equation 4.2 or LMR using equation 4.3. In this work Poisson's ratio is derived from velocity method.

$$\sigma = \frac{\left(\frac{Vp}{Vs}\right)^2 - 2}{2\left(\frac{Vp}{Vs} - 1\right)}. \quad (4.2)$$

$$\sigma = \frac{\lambda\rho}{2\,(\lambda\rho+\mu\rho)}. \quad (4.3)$$

Figure 4.7 shows the general relationship between Poisson's ratio and Vp/Vs ratio. Reservoir intervals have low in both Vp/Vs ratio and Poisson's ratio. Sand has lower Poisson's ratio than shale due to low Vp/Vs ratio of quarts in comparison with other minerals. Poisson's ratio measure of incompressibility of fluids, rocks that have lower values of Poisson's ratio contain compressible fluids meanwhile rocks that have higher values of Poisson' ratio tend to contain uncompressible fluid like water or shale.

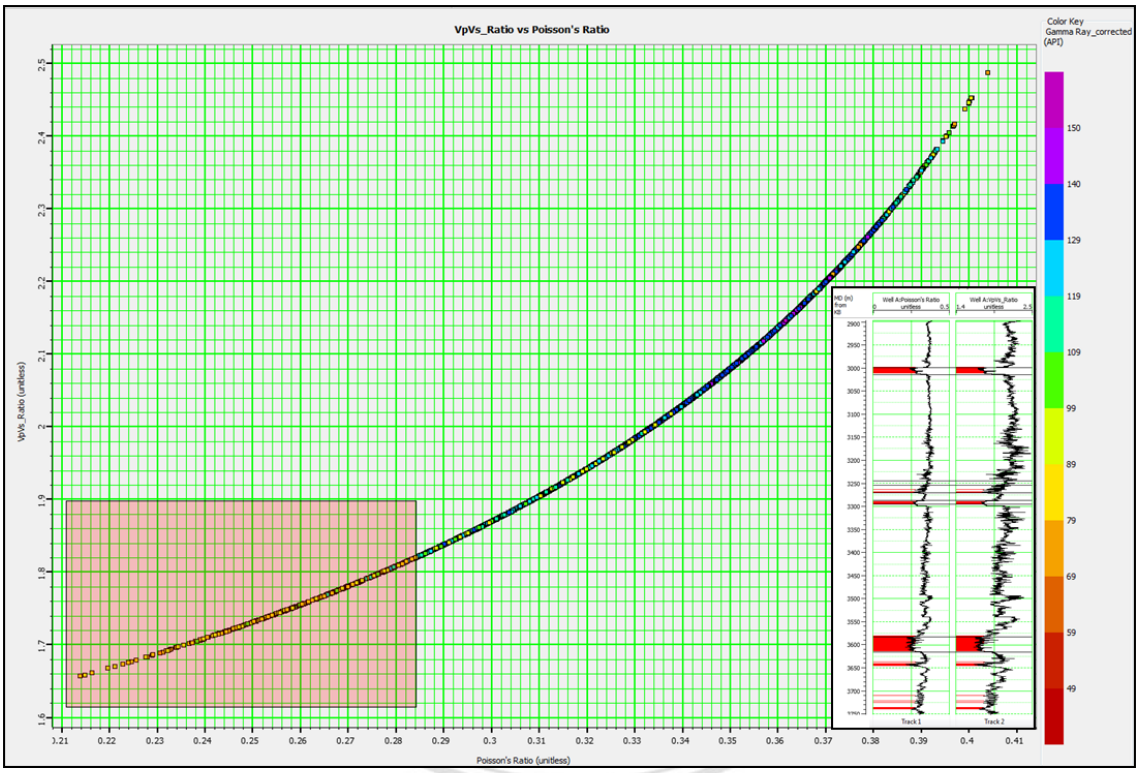

Figure 4.7: Cross plot of Poisson's ratio and Vp/Vs ratio. The red square polygon represents gas sand zone in the cross section.

Figure 4.8 shows the relationship between Poisson's ratio and velocity (P-wave). It is clearly that for a same value of velocity, Poisson's ratio of hard rock like consolidated sandstone is lower than poorly consolidated rock like shale. Especially for gas-bearing sandstone, Poisson's ratio shows values around 0.2 to 0.3 as shown in Figure 4.8 in comparison to other rocks. Poisson's ratio as well as velocity ratio is good lithology indicator.

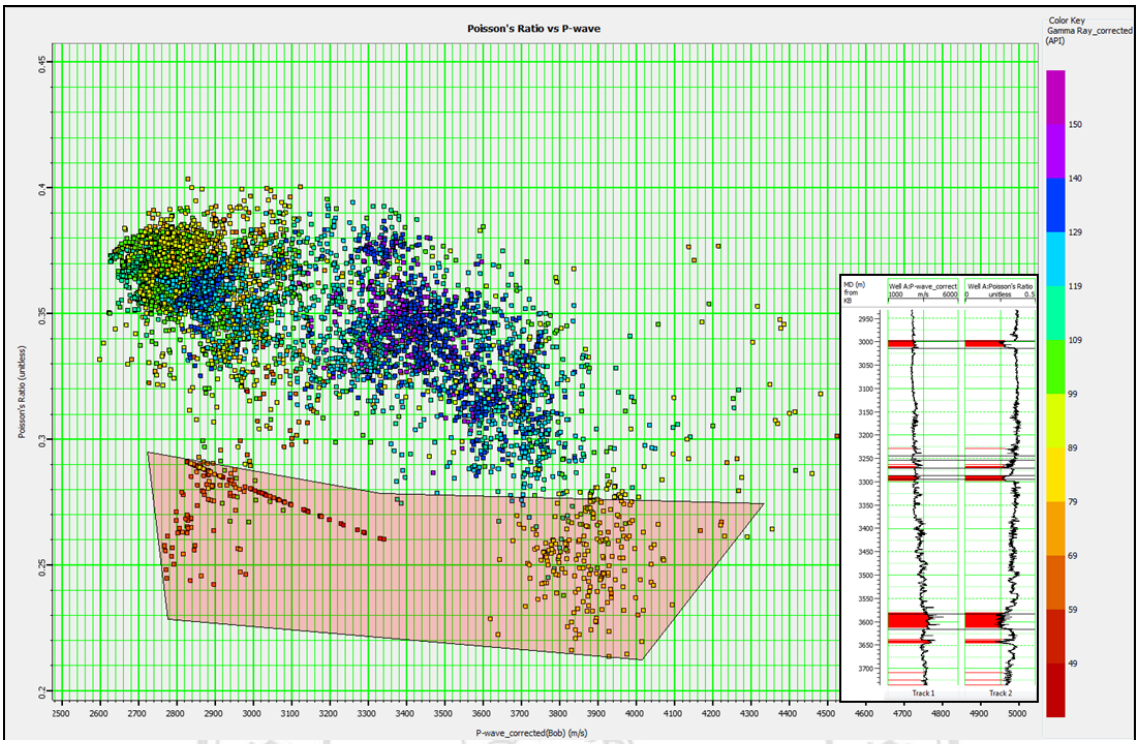

Figure 4.8: Cross plot of Poisson's ratio and P-wave velocity. The red rectangular polygon represents gas sand zone in the cross section.

Interactive Petrophysics (IP 3.5) is used in order to interpret the well logs data, generate other logs as well as highlight hydrocarbon bearing sand intervals in the Well A. Figure 4.9 shows the result of well logs interpretation for well A from 2800 m including three new logs shale volume (Vsh), effective porosity (Φe) and water saturation (Sw). Meanwhile Figure 4.10 and 4.11 show the zoom out results for two main reservoir intervals UMA15 and MMF30 accordingly.

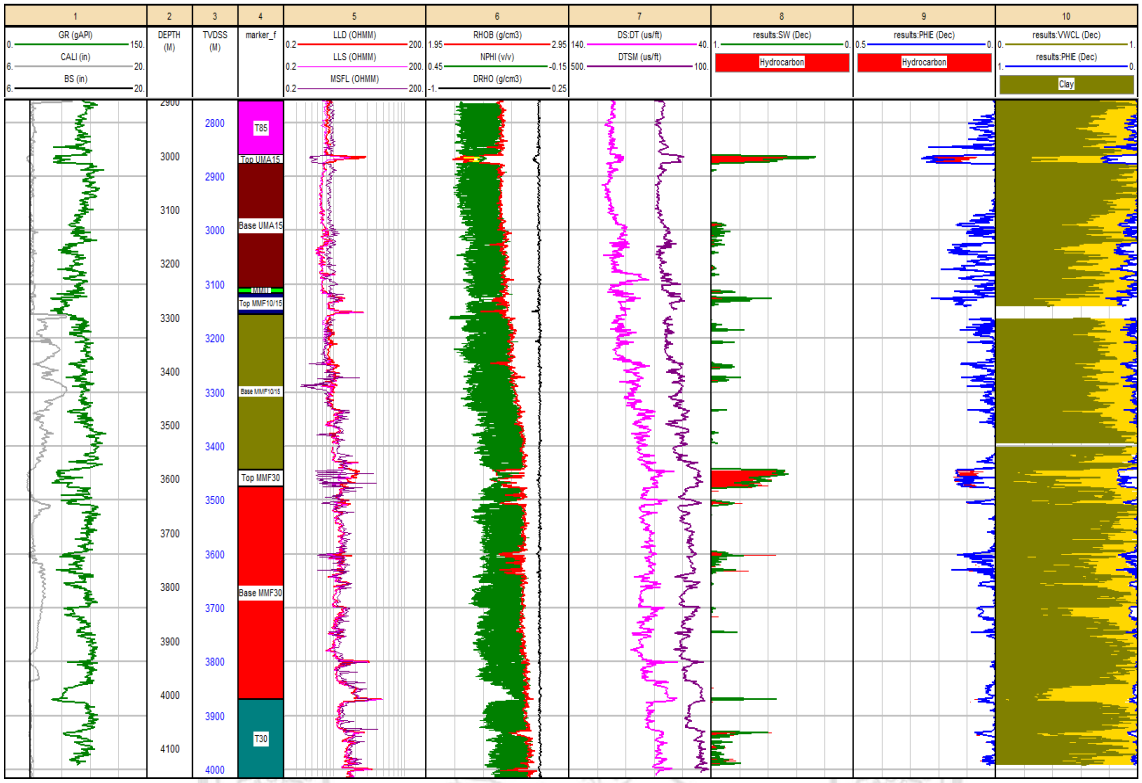

Figure 4.9: Result of well logs interpretation for Well A.

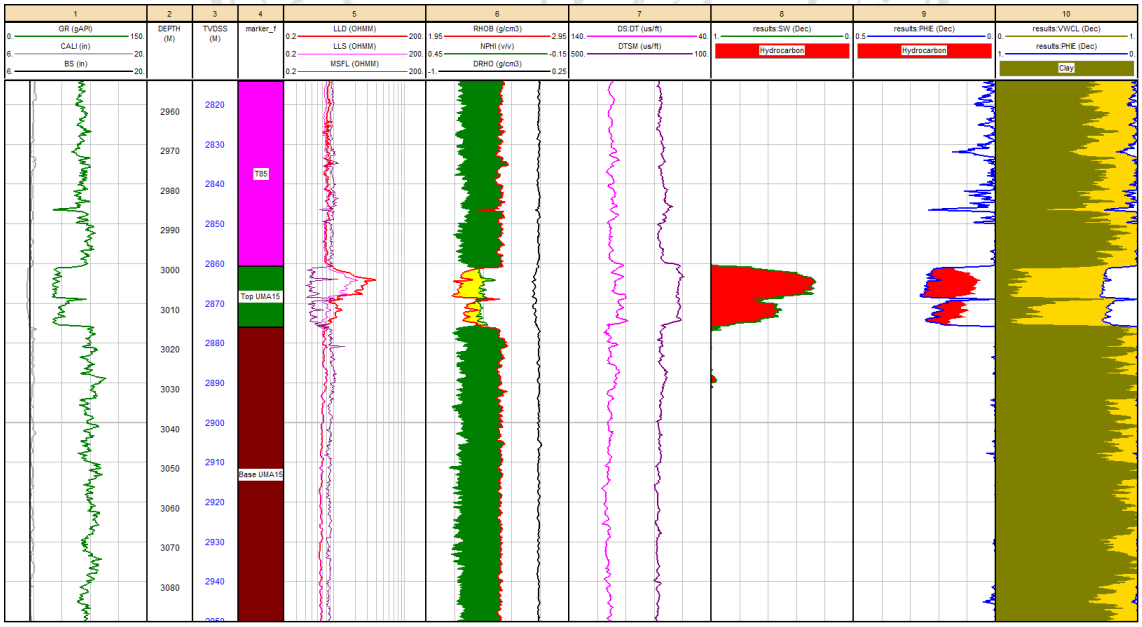

Figure 4.10: The zoom in results for reservoir interval UMA15.

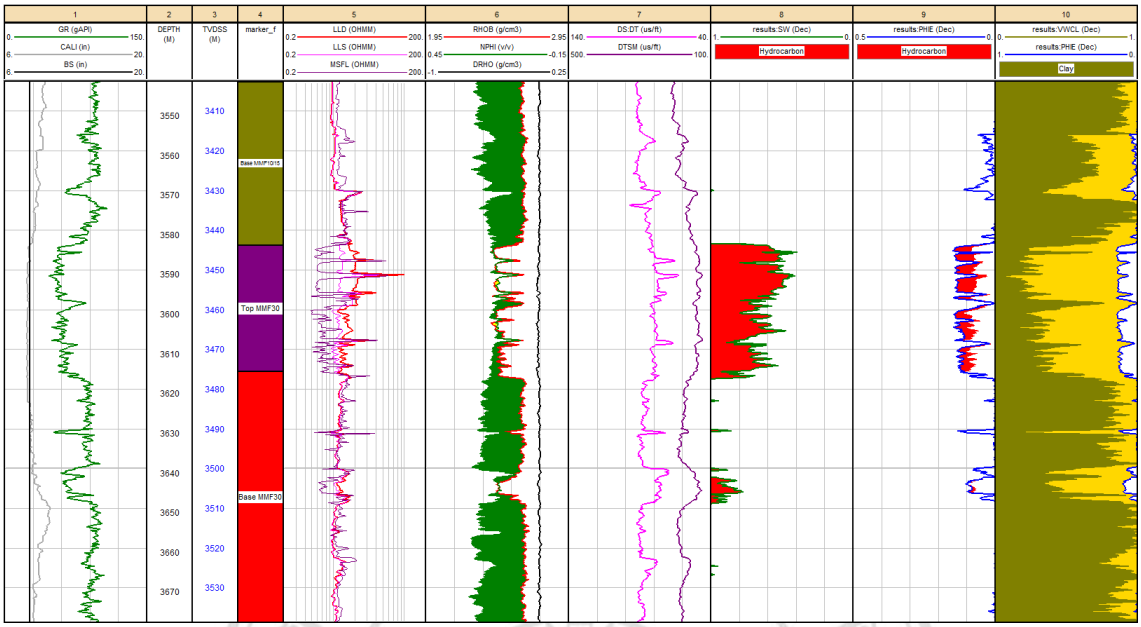

Figure 4.11: The zoom in results for reservoir interval MMF30.

4.3.3 Shale Volume (Vsh)

Shale volume (Vsh) is an important parameter in petrophysical analysis. Clay type and shale volume are affected not only on porosity but also on water saturation. There are many ways to determine the volume of shale. In this study, Vsh is estimated from Gamma Ray using linear equation:

$$GR = \frac{GR - GR_{sand}}{GR_{shale} - GR_{sand}}. \quad (4.4)$$

GR_{sand} and GR_{shale} are chosen for UMA15 reservoir interval are 55 API and 90 API while GR_{sand} and GR_{shale} are chosen for MMF30 reservoir interval are 60 API to 95 API. Vsh log is shown in track 10 in Figure 4.9.

4.3.4 Porosity from Density and Neutron

Porosity is the pore volume per unit volume of formation; it is the fraction of the total volume of a sample that is occupied by pores or voids (Schlumberger, 1972). It is represented by Greek letter, Φ and expressed as:

$$Porosity, \emptyset\ (\%) = \frac{volume\ of\ pores}{total\ volume\ of\ rock} \times 100\%. \quad (4.5)$$

There are two types of porosity in the rocks which are total porosity and effective porosity. The total porosity term includes all pore spaces, interconnected or not while the effective porosity term includes interconnected pores which allow the flow of fluids.

Porosity has a critical role to play in the evaluation of reserves and can be measured in many different ways. Note that the density log tools do not measure the porosity directly (Schlumberger, 1972). Neutron and density logs are affected in opposite directions by hydrocarbon (neutron gives low values while density gives high values) and by shale content (neutron gives high values while density gives low values). Thus, using the two logs together generally gives a successful correction for both effects. The equations for calculating porosity using density log and neutron log are expressed respectively as:

$$\emptyset_{density} = \frac{\rho_{matrix} - \rho_{log}}{\rho_{matrix} - \rho_{fluid}} - V_{sh} \frac{\rho_{matrix} - \rho_{shale}}{\rho_{matrix} - \rho_{fluid}}, \qquad (4.6)$$

where

ρ_{log}: Density from log (g/cc),

ρ_{matrix}: Matrix density (g/cc),

ρ_{shale}: Shale density of a nearby shale (g/cc),

ρ_{fluid}: Fluid density (g/cc),

Vsh: Volume of shale.

$$\emptyset_{neutron} = \emptyset_N - Vsh * \emptyset_{N_{shale}}, \qquad (4.7)$$

where

Φ_N: Neutron porosity from log,

Φ_{N_shale}: Neutron porosity from nearby shale,

Vsh: Volume of shale.

The matrix density and fluid density used in Equation 4.7 are default value for brine and sandstone as 2.65 g/cc and 1.09 g/cc. The input density and neutron porosity values are taken from well logs data while volume of shale is estimated in above part. The porosities from density and neutron (Equation 4.6 and 4.7) are just total porosities that include clay-bound water, free water and hydrocarbons. Therefore, to calculate effective porosity, quick look porosity equation would be used:

$$\emptyset_e = \sqrt{\frac{\emptyset_{De}{}^2 + \emptyset_{Ne}{}^2}{2}}, \qquad (4.8)$$

where

Φ_{Ne}: Porosity corrected from neutron log,

Φ_{De}: Porosity corrected from density log,

Φ_e: Effective porosity.

The effective porosity is shown in track 9 and 10 (Figure 4.9). It is then used as input parameters for estimating water saturation.

4.3.5 Water Saturation (Sw)

Water saturation is the amount of pore volume in a rock that is occupied by formation water; it is represented by a decimal fraction or percentage (Asquith,G. et al.,2004). In this study, the Sw log is mainly used in the fluid replacement modeling to construct AVO synthetic models later in the next chapter. In this study, because two main the reservoirs are not clean sand, it is quite not reasonable to use clean sand method like Archie equation to calculate the water saturation. It is necessary to use formulas involving volume and resistivity of shale into calculation. Therefore, Indonesian equation (Equation 4.9) is used to calculate water saturation in the Well A:

$$S_W = \left[\frac{\frac{1}{R_t^{0.5}}}{\frac{V_{sh}^{1-Vsh/2}}{R_{sh}^{0.5}} + \frac{\emptyset^{m/2}}{(a*R_w)^{0.5}}} \right]^{2/n} , \quad (4.9)$$

where

a: Tortuosity factor,

m: Cementation exponent,

n: Saturation exponent,

Φ=Φe: Effective porosity,

Vsh: Volume of shale,

Rsh: Resistivity of shale formation,

Rw: Resistivity of water formation,

Rt: True deep resistivity.

Note that some of input parameters are provided by the company from study of the wells near well A. In the Equation 4.9, based on SCAL result of Well A and the wells nearby, a,m and n parameters are determined as 1, 1.85 and 1.85 respectively for UMA15 and 1, 2 and 2 respectively for MMF30 (this parameters are provided by the company). Φ is porosity that used the effective porosity log estimated from density and neutron porosity logs above, R_t is true resistivity of the formation which is measured by the resistivity LLD log from well dataset. The input parameters R_w is estimated from water saturated sandstone interval by the resistivity temperature conversion with input temperature of 25^o C and water salinity of 30,000 ppm salinity than was taken from

water samples analysis results of adjacent wells (this parameters are provided by the company). The last unknown input parameter for Indonesian's equation is R_{shale} which is estimated in the thick shale interval, R_{shale} values vary from 1 Ohmm to 4.3 Ohmm with different shale intervals along the well A. After calculation, the Sw log is shown in track 8 in Figure 4.9. It is obvious that the reservoir UMA15 interval has water saturation value of 0.3 to 0.7 and the reservoir MMF30 interval has water saturation value of 0.5 to 0.8.

4.4 Time – Depth Conversion

Well to seismic ties is important because of many reasons: to provide Time – Depth conversion, to understand wavelet phase, to understand seismic resolution, to check validity of seismic data processing, to tie significant geological markers to seismic data and to decide what to pick – Peak, Through or Zero Crossing. In this chapter, the time – depth conversion and tie geological markers to seismic data is discussed, the rest of reasons are discussed in chapter 5. Time – depth conversion is the first and one of most important part in well tie seismic procedures. Because seismic data is acquired in time domain and wells data is measured in depth domain, in order to interpret and describe geology of the subsurface accurately, it is essential to do depth to time conversion before doing seismic – well tie.

Because vertical seismic profiles (VSP) data is available in Well A, it is integrated with original P-wave sonic log of Well A to determine the time – depth function. One thing should be considered before carrying out log calibration is dispersion of velocity. The Sonic log uses high frequencies (almost 20 kHz) at small distances while surface seismic like VSP have longer transmission paths and low frequencies. Therefore, the sonic log needs to be up-scaled to calibrate with the seismic velocity; fortunately, this process is done automatically by Hampson Russell software. Log calibration is conducted using Checkshot Correction function in Hampson Russell software.

In the check shot correction function, a drift curve measures the discrepancy between the checkshot data and time – depth curve from the integrated sonic log. The differences in times between P-wave sonic log and checkshot (in this case is VSP data) are solved using different types of interpolation like linear, spline and polynomial. The linear

interpolation with knee points is applied where there are lithology changes or unconformities. At that location, there are changes in velocities and the linear interpolation help avoid some bad reflections in the calibrated sonic log. The spline interpolation type is applied when VSP data are available, for checkshot data, the result should be QC again. The polynomial interpolation type is applied where there is simple compaction trend in basin fill sequences (Simm & Bacon, 2014). Because of the complication in lithology variations in the Well A that is mentioned in the geological completion report of the Well A, the linear interpolation type is applied for drift curve to determine the T - D relationship for Well A (Figure 4.12). After that, the time – depth curve will be corrected using the drift curve. In well tie process, the original P-wave velocity log is used to match well to seismic instead of the calibrated P-wave velocity log. This is because of the better ties when using the original rather than the calibrated one.

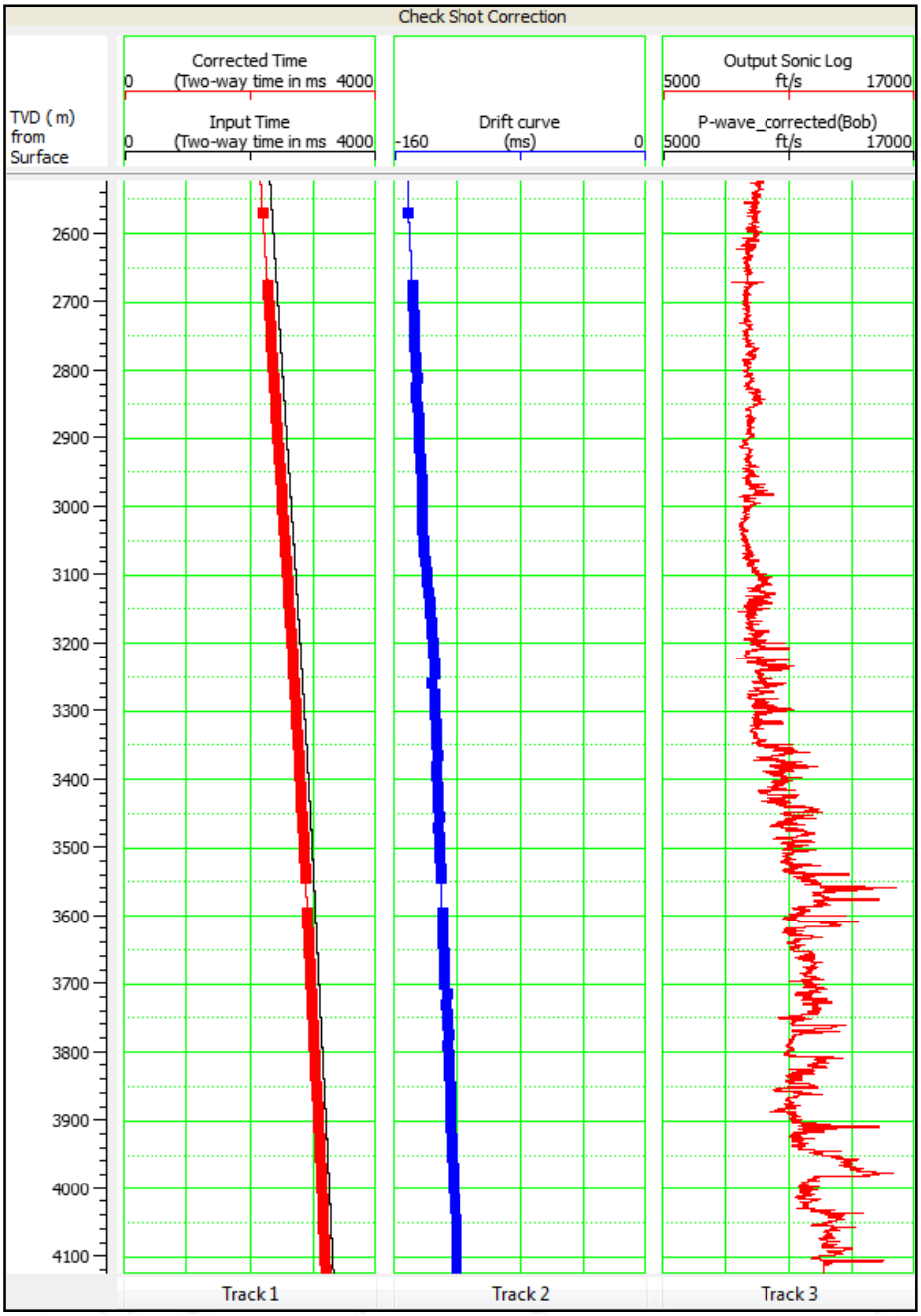

Figure 4.12: Log (depth – time) calibration using linear trends as drift function: track 1, black – Input T-D curve from sonic log, red – calibrated T-D curve; track 2, blue – drift curve fitted to the data using linear segments with knee points; track 3, black – original P-wave sonic log, red – calibrated P-wave sonic log.

After the calibrated time – depth relationship is achieved, average velocities and interval velocities are calculated depending on the time – depth relations of the original P-wave, VSP data and all interpolation types. The average and interval velocities are plotted versus depth (MD) to compare the time – depth relationship before and after checkshots

correction procedure (Figure 4.13 and 4.14). From the depth of 0 m to around 2600 m, the average velocities after checkshot correction for all types of interpolation fall between the average velocities of check shots data and original P-wave sonic log. This is because of there is no checkshot data in this depth. From the depth around 2600 m to total depth of 4155 m where the checkshot data have been measured, the average velocities of VSP data and all types of interpolation join together. It means at that location the time – depth relations have been corrected follow checkshot data. For the interval velocities in Figure 4.14, the interval velocities of checkshot data is lower and separated with the interval velocities of original P-wave sonic log and all types of interpolation because there is no checkshot until 2600 m. From 2600 m, the interval velocities of all time – depth relations join together.

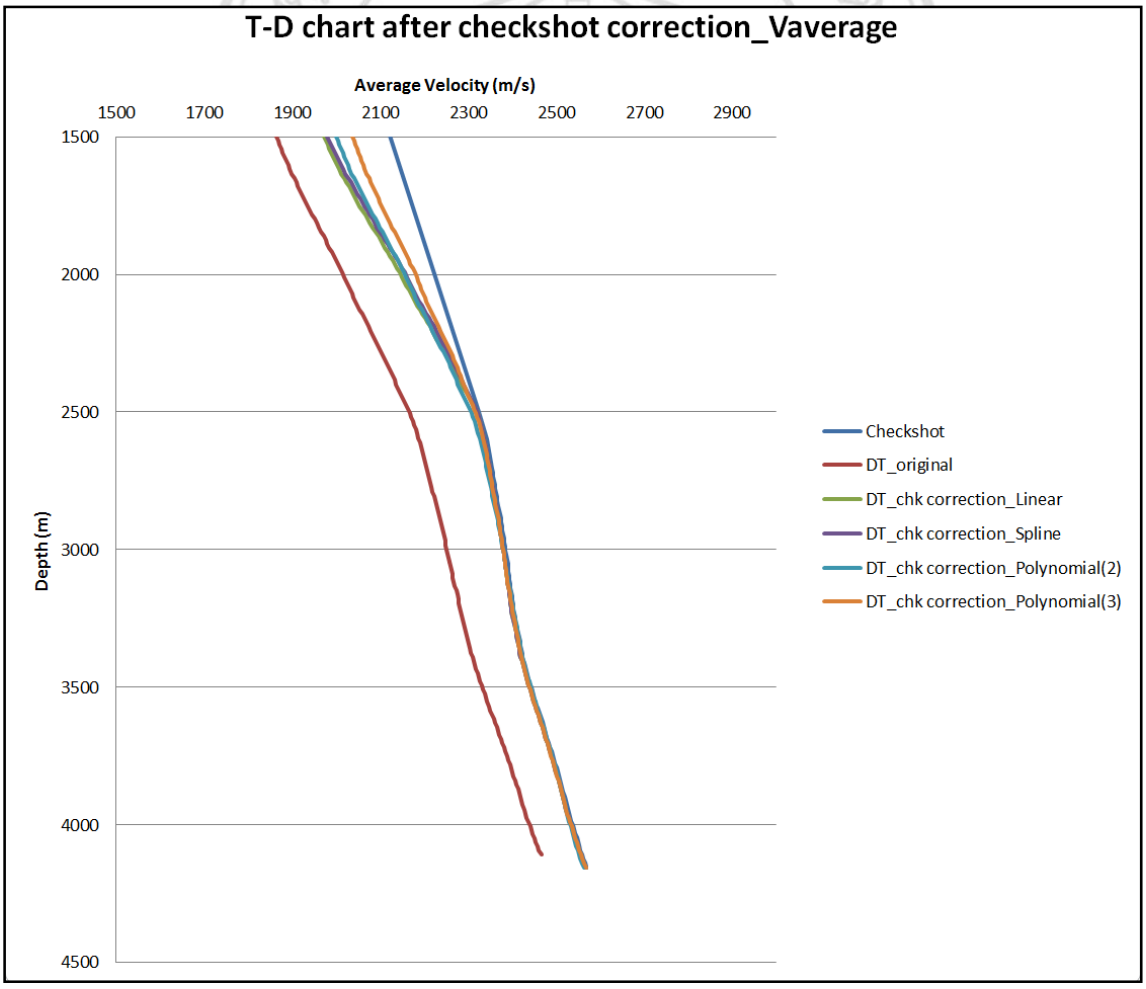

Figure 4.13: Plot of average velocity between different type of check shot correction.

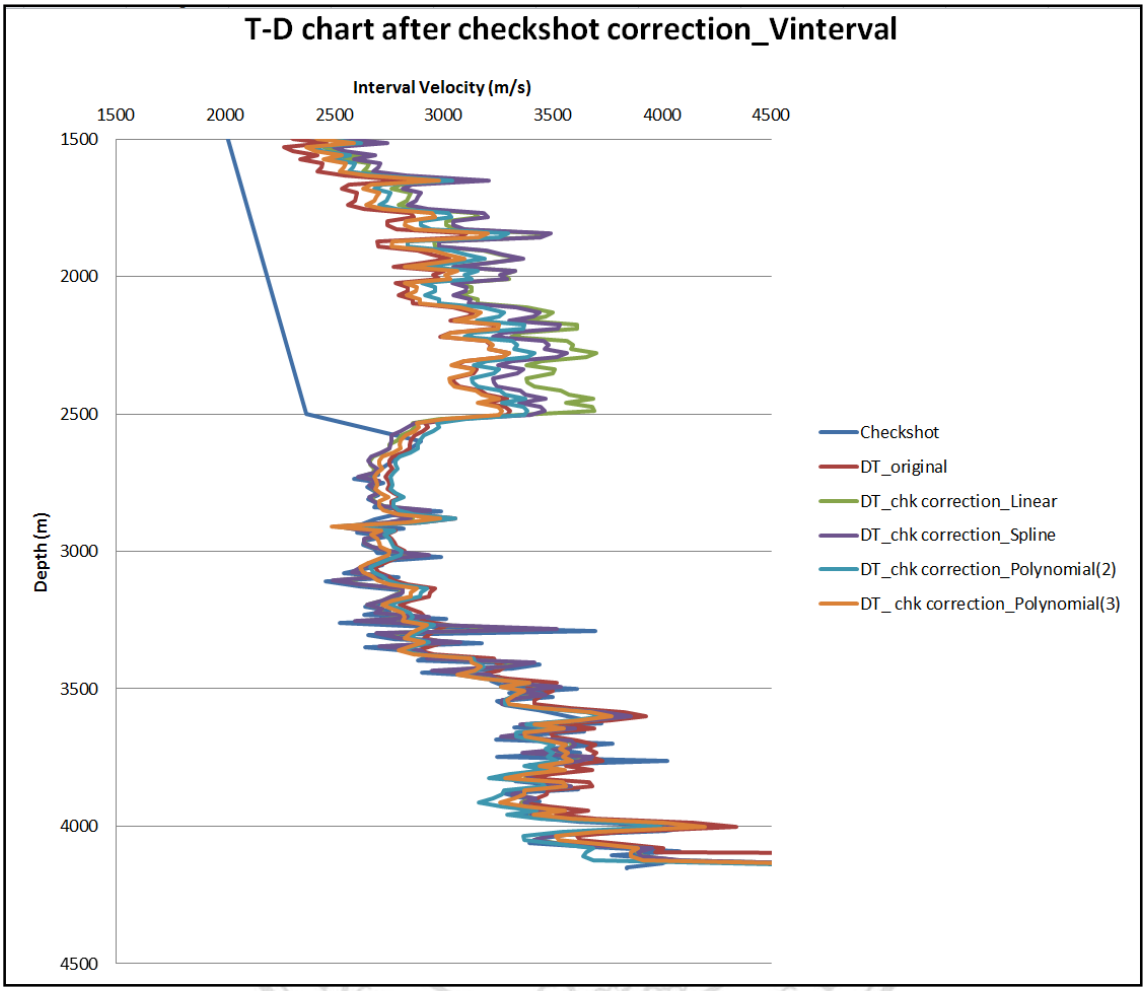

Figure 4.14: Plot of interval velocity between different type of check shot correction.

Figure 4.15 shows the result of the checkshot correction in time – depth relationship of the Well A. It is clearly that the geological markers in the Well A change the depth follow the time depth relations of the well. The markers position in the Well A after checkshot correction returned to their real position in the seismic data. Seismic horizons interpretation followed the geological markers is shown in the next part of this chapter.

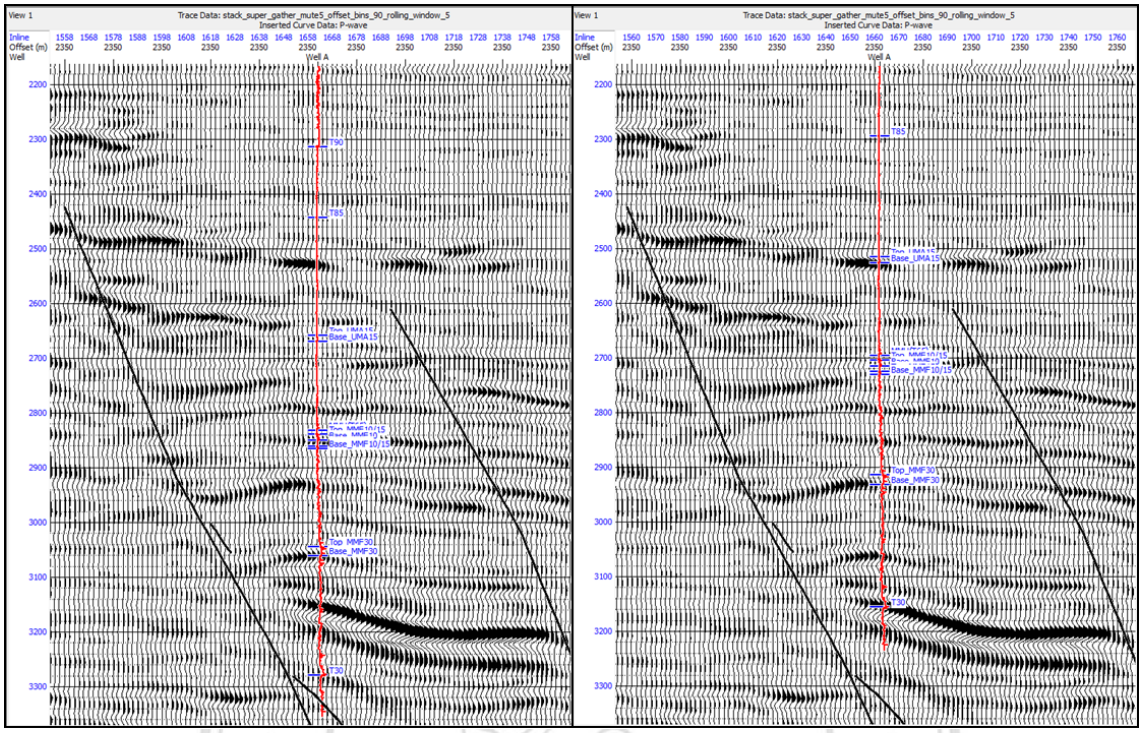

Figure 4.15: Well A before and after checkshots correction.

4.5 Seismic Interpretation

Primary goal of seismic interpretation works in this chapter is describing structural and amplitude information of 3D seismic volumes. Structural interpretation is carry out by integrating all available data, in this case seismic and well data, to build understanding about the picture of subsurface structure and stratigraphy of the prospect. In addition, amplitude information provides additional data that can be used for advanced interpretation seismic data like reservoir characterization study. For these purposes, logs and formation tops of Well A integrating with full offset stack 3D seismic data are used. Summary of interpretation processes as follow (not in order):

- Import well and seismic data into software.
- Establish well ties/select starting point for interpretation (shown in part 4.4).
- Interpret/Correlate horizons and faults integrating with seismic attributes.
- Mapping and contouring time structure map.
- RMS amplitude attributes.

Kingdom Suite 8.8 software has been used for seismic interpretation while Petrel 2013 software has been used for generating seismic attributes volumes, seismic attributes are extracted and represented in Kingdom Suite 8.8 software.

4.5.1 Horizons Interpretation

Seven (7) horizons were picked on 3D seismic volume between the time of interval of 2100 ms and 3900 ms (Figure 4.16 and 4.17). The 6 horizons were picked following the formation tops of the Well A using the corrected Time – Depth chart from sonic log after well to seismic ties as shown in part 4.4 above, excepting the deepest horizon T10 was picked as top of Oligocene period. Formation tops information of the Well A provided by the company is shown in Table 2.1. Names of the 7 horizons follow the formation tops, colors and ages of those horizons are shown in Table 4.1.

Table 4.1: Seven horizons were picked on seismic data.

Horizons	Colors	Ages of boundary
T90	Sky Blue	Top of Early Pliocene
T85	Violet	Top of Late Miocene
Top UMA15	Yellow	Top of reservoir UMA15
T65	Green	Top Middle Miocene
Top MMF30	Dark Cyan	Top of reservoir MMF30
T30	Pink	Top Early Miocene
T10	Orange	Top Late Oligocene

Horizon T10 was picked at around 3200 ms and 3750 ms at positive reflectivity (peak), low reflection continuity and low to medium amplitude. The reflection configuration of horizon T10 is mainly sub-parallel and hummocky, frequency of seismic data is low. Horizon T30 was picked at approximately from 2800 ms to 3600 ms at positive reflectivity (peak), low to high continuity and medium to high amplitude. Sub-parallel is major as reflection configuration and frequency is low. Horizon Top MMF30 was picked at around 2700 ms to 3100 ms at negative reflectivity (trough), characterized by medium to high amplitude and medium to high continuity. The major reflection configuration of horizon Top MMF30 is sub-parallel and seismic frequency is low. Horizon T65 was picked at around 2500 ms and 2900 ms at negative reflection (trough),

medium to high continuity and moderate amplitude. Clinoform types as sigmoid and oblique and parallel are internal reflection configuration, seismic frequency at this depth is high. Horizon Top UMA15 was picked at approximately 2450 ms to 2650 ms at negative reflection (trough), characterized by low continuity and low to high amplitude. The reflection configuration of horizon Top UMA15 is hummocky, seismic frequency is high. Horizon T85 was picked at around 2300 ms and 2400 ms at positive reflectivity (peak), characterized by discontinuous reflectivity and low to high amplitude. The reflection configuration of horizon T85 is hummocky and deformed, seismic frequency is high. Horizon T90 was picked at around 2100 ms to 2200 ms at negative reflectivity (trough), characterized by low to medium continuity and low to high amplitude. The reflection configuration of horizon T90 is sub-parallel and hummocky, seismic frequency at this depth is high.

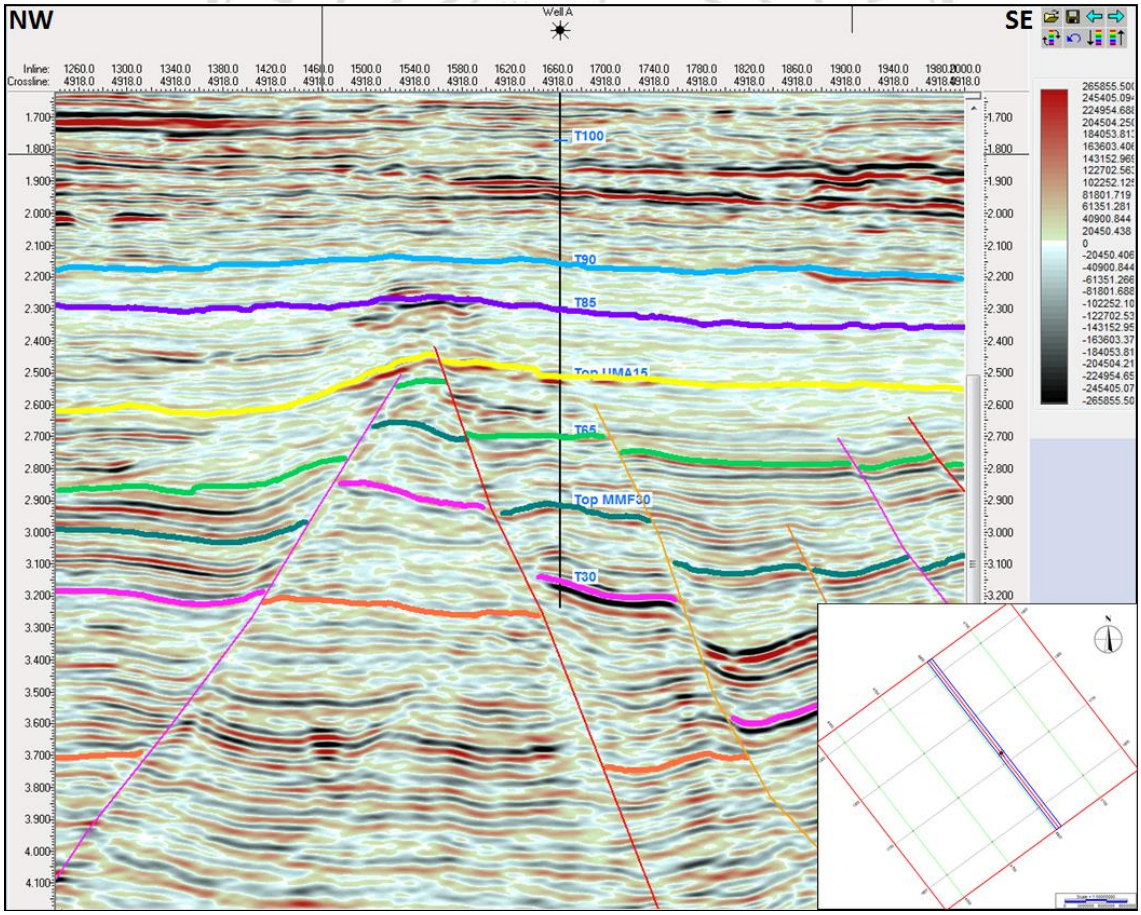

Figure 4.16: Crossline 4918 cross the Well A. Seven horizons were picked on seismic data.

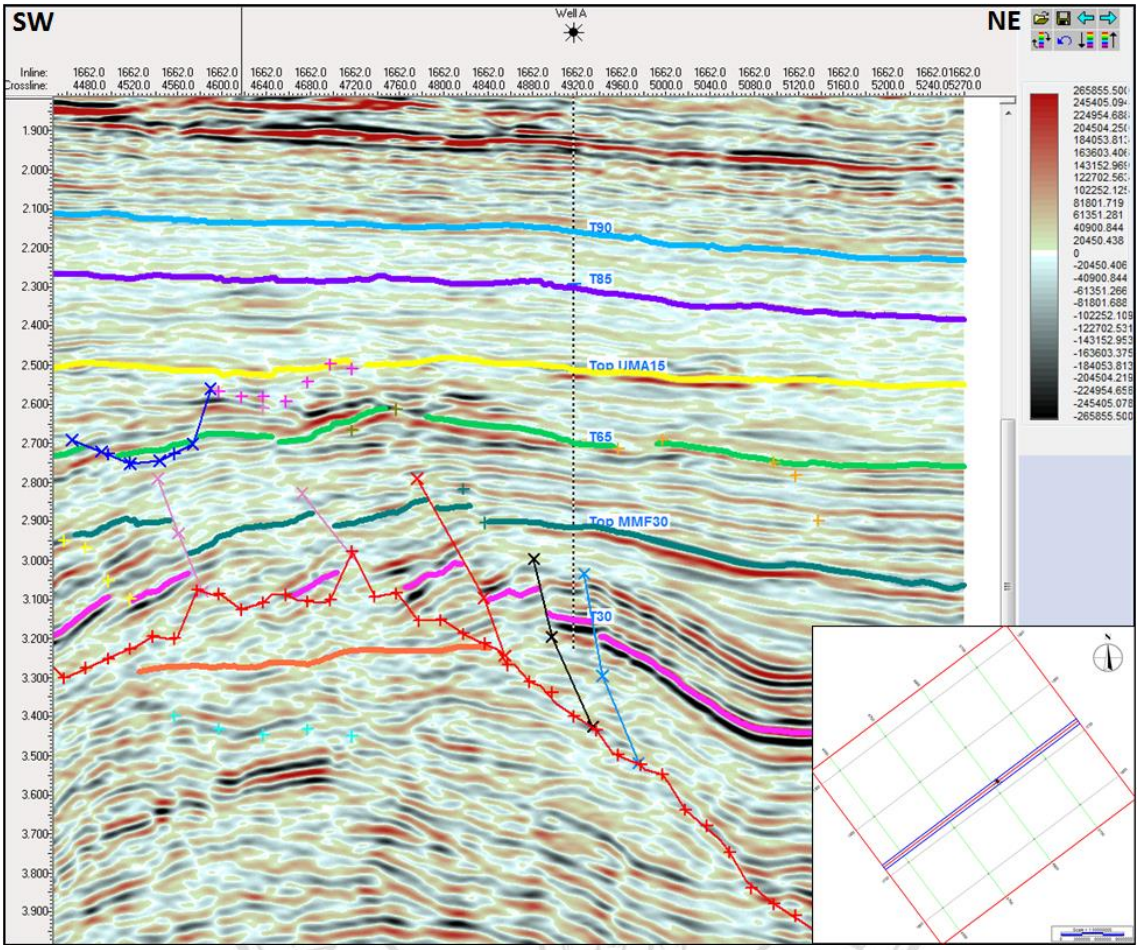

Figure 4.17: Inline 1662 cross the Well A. Seven horizons were picked on seismic data.

The horizons were identified at Well A's location firstly and interpreted to all the 3D seismic volume with guiding of faults. These interpreted horizons show the structural and stratigraphic features at well location and whole are in the seismic data. Horizon picks are very important for building initial inversion model in the next chapter.

4.5.2 Faults Interpretation

All the major faults in the seismic data are picked to guide the horizons interpretation and define the geometrical of structure highs and trapping mechanism for hydrocarbons accumulations. The structural framework was done by picking assigned fault segments on the crossline sections (Figure 4.18 and 4.19) of seismic data and the faults surfaces appearing on the corresponding Inline (Figure 4.20). Interpretation faults using just the inlines and crosslines in the seismic data is not enough especially when the event strikes are parallel to the faults and the horizontal section does not show the faults well. It is essential to integrate seismic attribute to improve the recognition of faults in seismic

volumes. Coherence seismic attributes, therefore, will allow faults mapping easier especially for subtle faults. The Petrel software calls Coherence attributes as Variance seismic attributes, the Variance attribute is the estimation of local variance in seismic reflectivity.

In the seismic data, thirty faults have been mapped and all of those are normal faults, faults related to the main reservoir are focused and shown from Figure 4.18 to Figure 4.20. The Variance attribute is generated at 2980ms. The Variance attribute parameters are filter window size of 3 as inline and cross line range and 15 ms as vertical smoothing length. These parameters are chosen after experiment of various parameters in order to achieve the good attributes images to recognize small and subtle faults in study area. In the faults zones, high amplitudes of Variance attributes indicate the location of termination seismic reflection while low amplitude show continuous reflectivity.

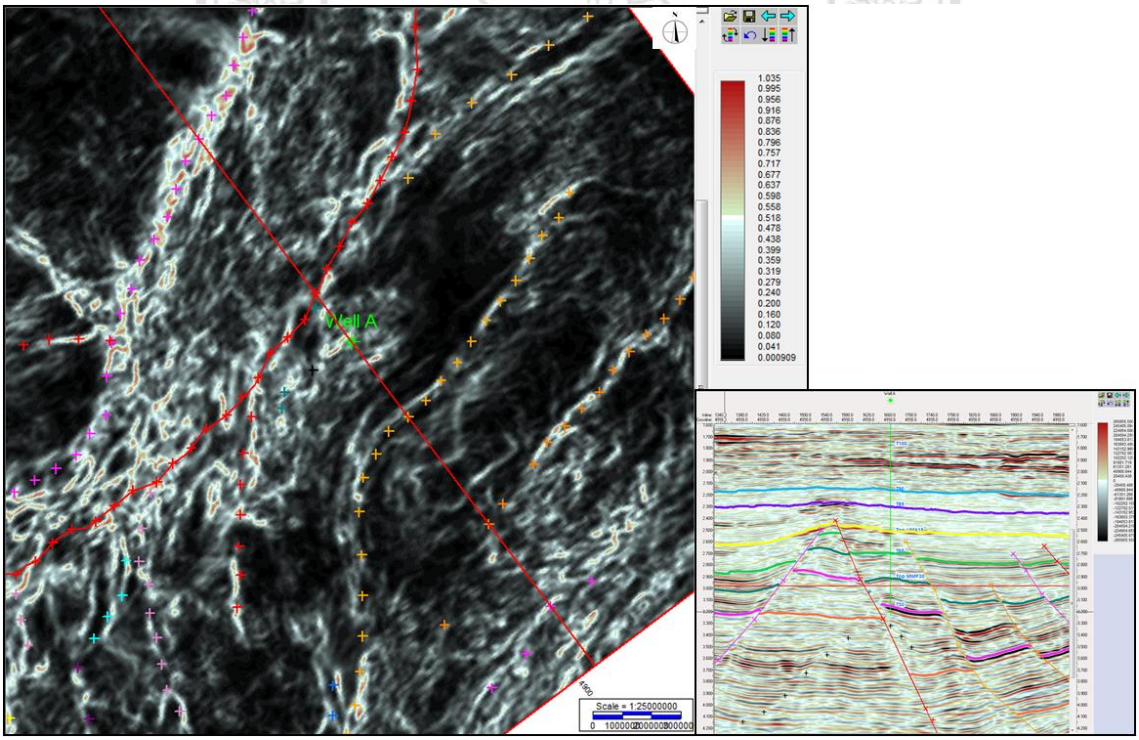

Figure 4.18: Variance attribute at time slice 2980 ms. Cross line 4918 through the Well A shows the horizons and faults represented in the time slice 2980 ms.

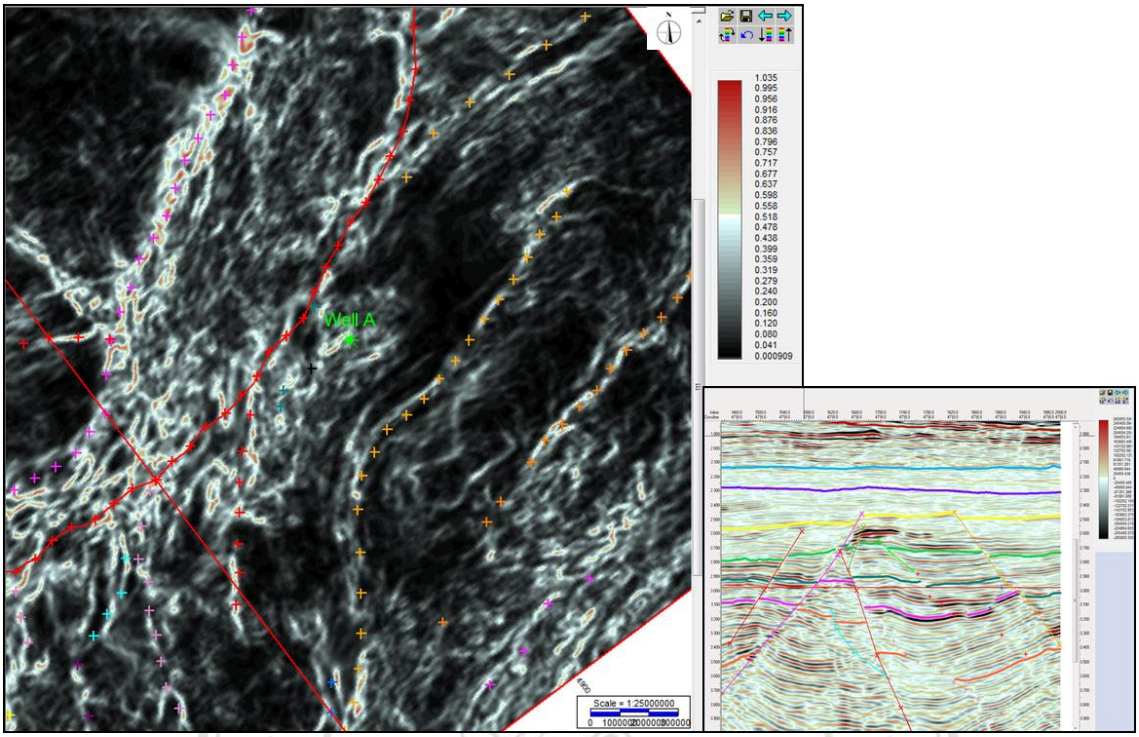

Figure 4.19: Variance attribute at time slice 2980 ms. Cross line 4718 shows the horizons and faults represented in the time slice 2980 ms.

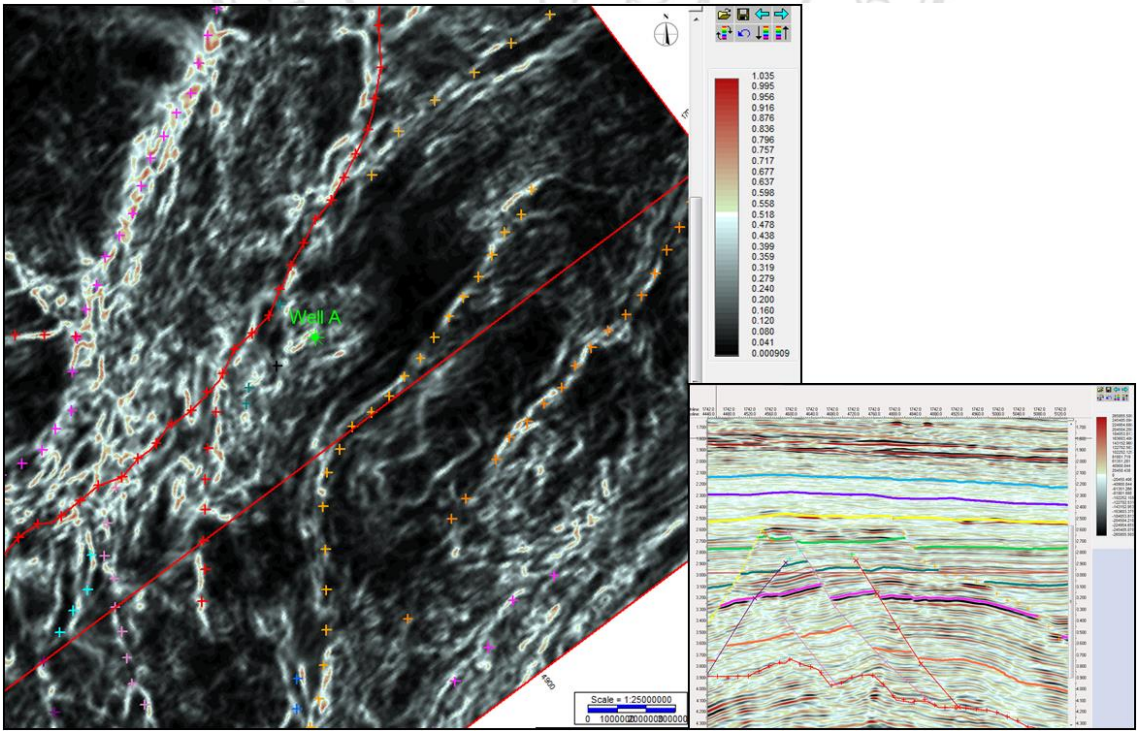

Figure 4.20: Variance attribute at time slice 2980 ms. Inline 1742 shows the horizons and faults represented in the time slice 2980 ms.

4.5.3 Seismic Amplitude Attributes

Besides the Variance attributes as showing in part 4.5.2 above, RMS Amplitude seismic attribute is used to describe hydrocarbon reservoir and enhance reflectivity information of the reservoir. RMS Amplitude computes Root Means Squares on instantaneous trace samples over a specified window, a window length parameter is defined by the number of the samples (Schlumberger, 1998). The RMS Amplitude attribute, in other words, emphasizes the variations in acoustic impedance over a selected sample interval. It is a statistical measurement of the amplitude variations over seismic dataset, the equation to calculate RMS Amplitude attribute in Petrel software is:

$$x_{RMS} = \sqrt{\frac{{x_1}^2+{x_2}^2+\cdots+{x_n}^2}{n}}. \quad (4.7)$$

The RMS Amplitude attribute is a post-stack attribute, this means it is applied for post-stack seismic data. In this independent study, the RMS amplitude is extracted from near-, mid- and far-angle stack volumes in the time intervals from 3 ms above to 3 ms below along two top reservoirs horizons Top UMA15 and Top MMF30. The used filter window is small due to the reservoir interval is quite thin around 15 m for UMA15 reservoir and 33 m for MMF30 reservoir and to highlight the amplitude of reflectivity more clearly. The RMS Amplitude maps of two horizons applied for near-, mid- and far- angle stacks is shown in Figure 4.22 to Figure 4.26.

The RMS amplitude along horizon Top UMA15 shows significant variations from near-angle stack to far-angle stack volumes. For the near-angle stack in Figure 4.21, high amplitude seismic reflectivity distributes in whole the map especially for the center and the west part of the study area. The amplitude around Well A's location shows low amplitude For the mid-angle stack in Figure 4.22, the high amplitude in the west part of the study area is almost disappeared and the high amplitude in the center part increase and reveal more clearly. Amplitude in the Well A's location increases. Figure 4.23 shows the RMS amplitude for the far-angle stack, the high amplitude just reveal in the center around the Well A's location and especially the very high amplitude is shown in the south part of the Well A's location. The amplitude of reflectivity along horizon Top UMA15 points out clear the amplitude variations from low amplitude in the near-angle stack to high amplitude in the far-angle stack. AVO of horizon Top UMA15 is discussed in chapter 5.

Similar to the RMS amplitude along horizon Top UMA15, the RMS amplitude along horizon Top MMF30 shows significant variations from near-angle stack to far-angle stack volumes. For the near-angle stack in Figure 4.24, the amplitude reflectivity shows low amplitude in the Well A's location and the East and North East part of study area. While high amplitude appears in the South, West and North West part of study area. For the mid-angle stack as shown in Figure 4.25, the amplitude reflectivity of whole study area decreases noticeably, the amplitude in the Well A's location is almost zero. Figure 4.26 shows the RMS amplitude for the far-angle stack, it is clearly that the amplitude reflectivity in the Well A's location and the East part of study area increase dramatically from zero amplitude to high amplitude, the rest of study area has very low of amplitude reflectivity. As a result, the amplitude of reflectivity along horizon Top MMF30 in Well A's location shows decrease in amplitude in near-angle stack and rapid increase amplitude in the far-angle stack. AVO of horizon Top MMF30 is discussed in chapter 5.

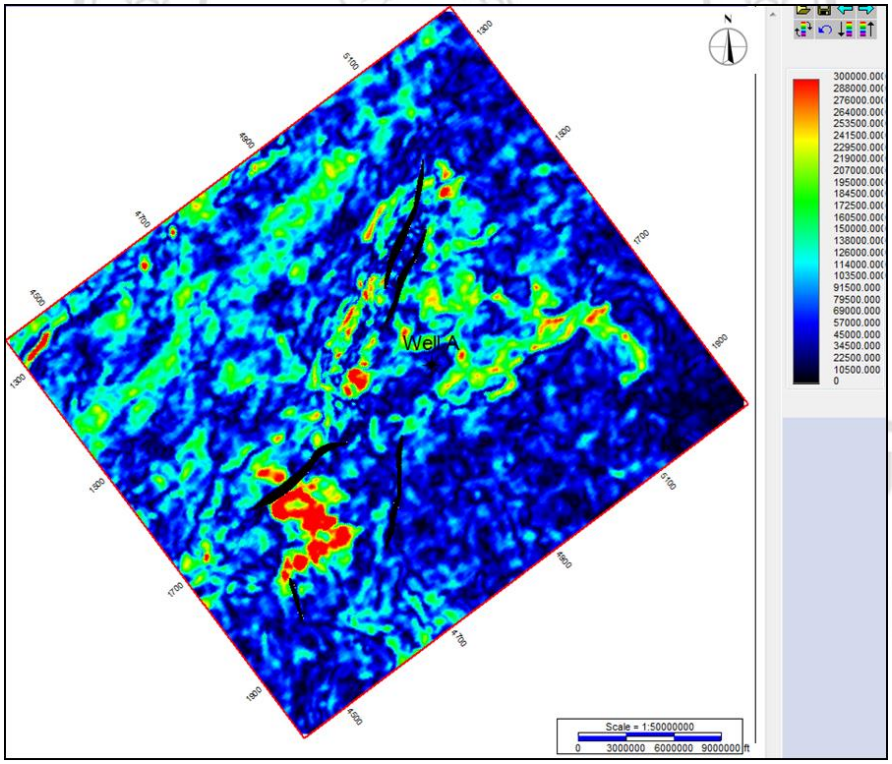

Figure 4.21: RMS Amplitude from near-angle stack volume along UMA15.

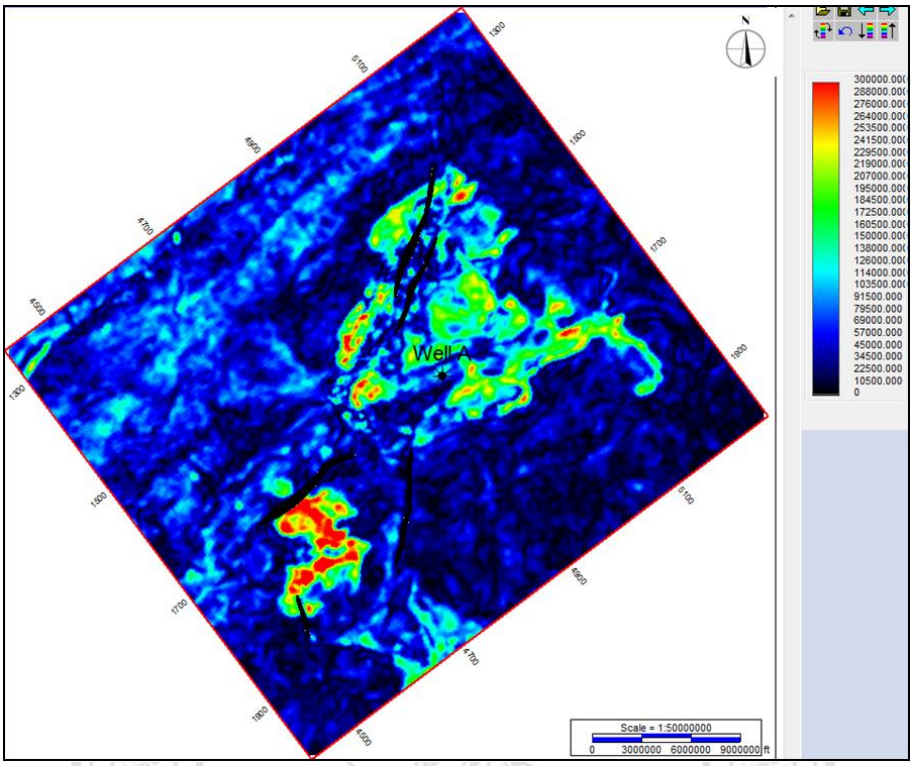

Figure 4.22: RMS Amplitude from mid-angle stack volume along UMA15.

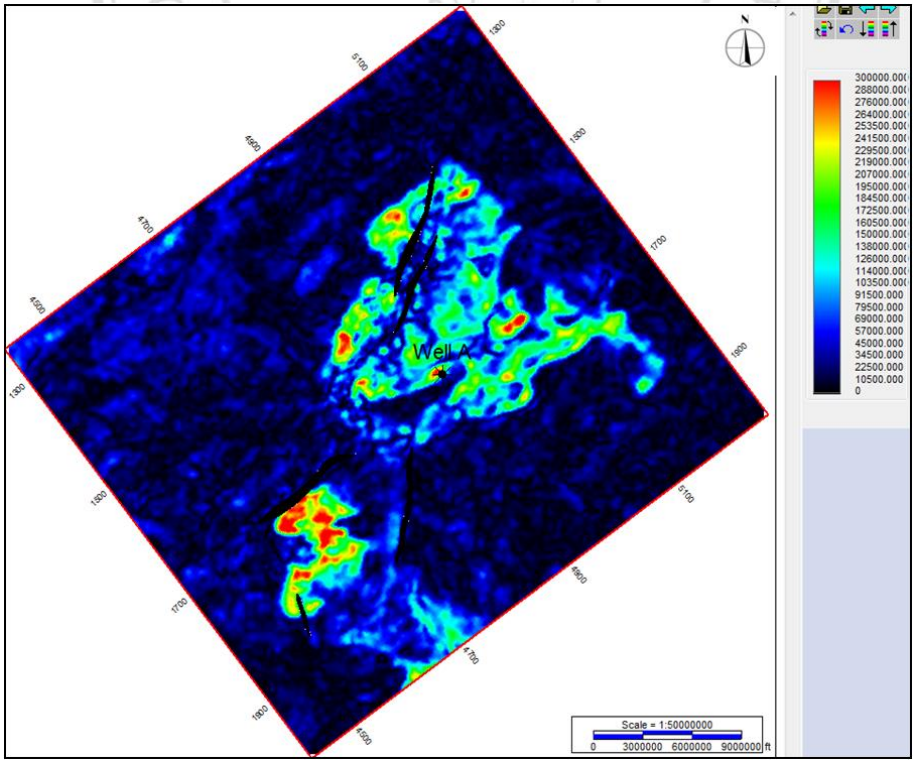

Figure 4.23: RMS Amplitude from far-angle stack volume along UMA15.

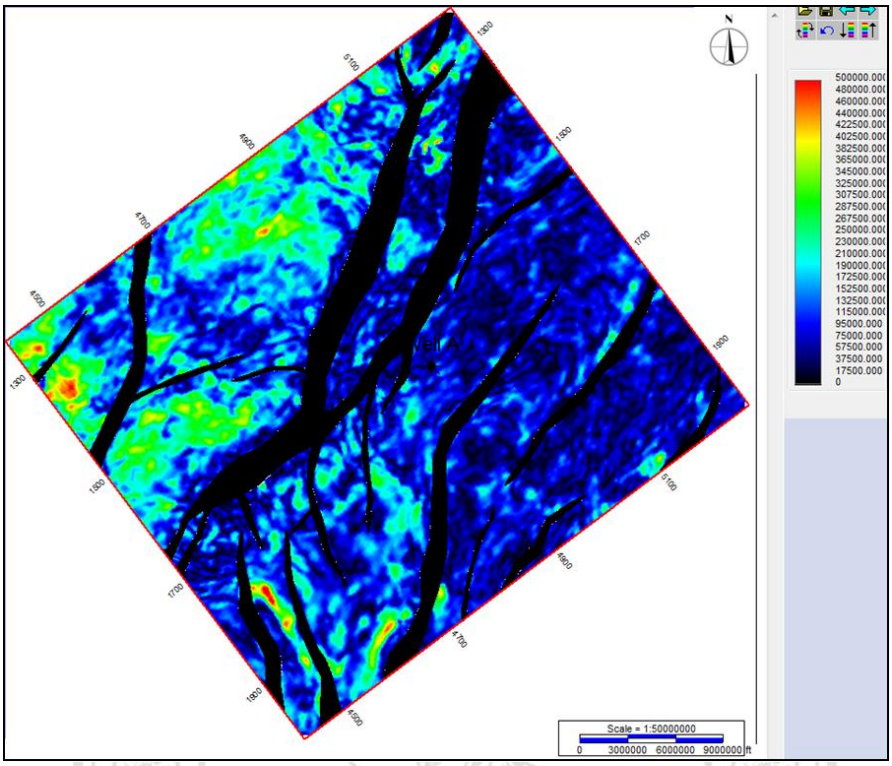

Figure 4.24: RMS Amplitude from near-angle stack volume along MMF30.

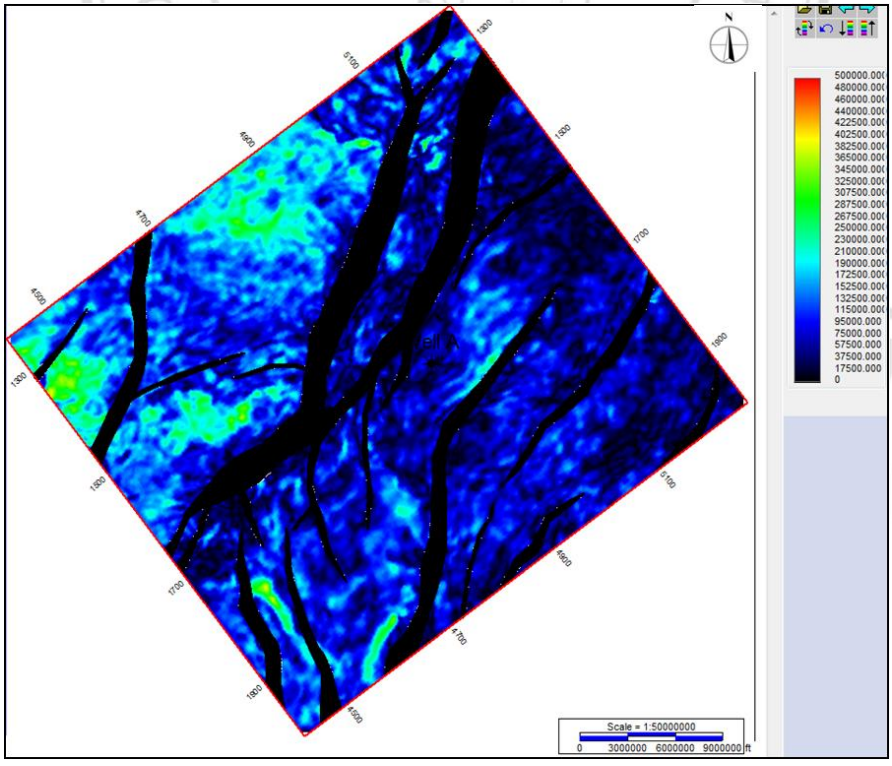

Figure 4.25: RMS Amplitude from mid-angle stack volume along MMF30.

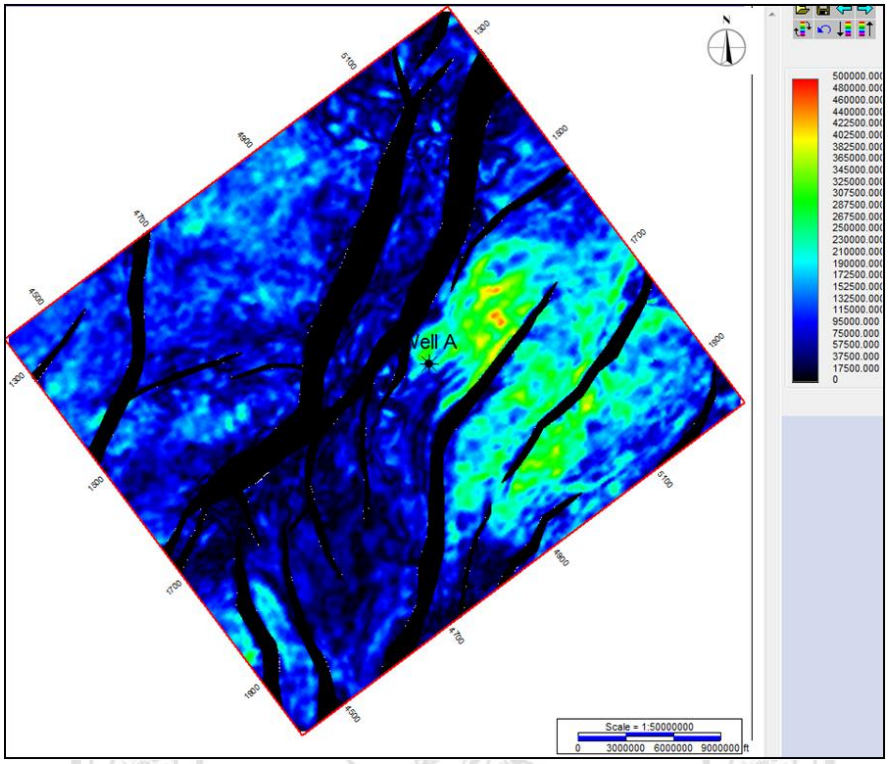

Figure 4.26: RMS Amplitude from far-angle stack volume along MMF30.

4.6 Time Structure Map

Time structure map represents the seismic image of the subsurface structure in time. Time structure maps of seven horizons including two top of reservoirs UMA15 and MMF30 are shown in Figure 4.27 to Figure 4.33.

The major fault trends of study area have North East – South West or North –South direction while minor faults have West – East direction. The minor faults are mainly the branches of main faults or small single faults. Number of faults and their displacements reduce from older horizon T10 (Top Oligocene) to horizon Top UMA15. The regional faults geometries from Figures 4.27 to 4.33 also suggest that the North East – South West faults are the oldest in the study area. They control the geological structure and trapping mechanism for the hydrocarbons.

The main high structure located in the center of study area is formed from the development of two main faults have direction of North East – South West. However instead of the horst targets, Well A is drilled in the flanks of the main high structure to explore the sand body Middle Miocene MMF30 and appraise the sand body UMA15 in

Upper Miocene as shown in time structure map of Top UMA15 and Top MMF30 (Figure 4.31 and Figure 4.29 respectively).

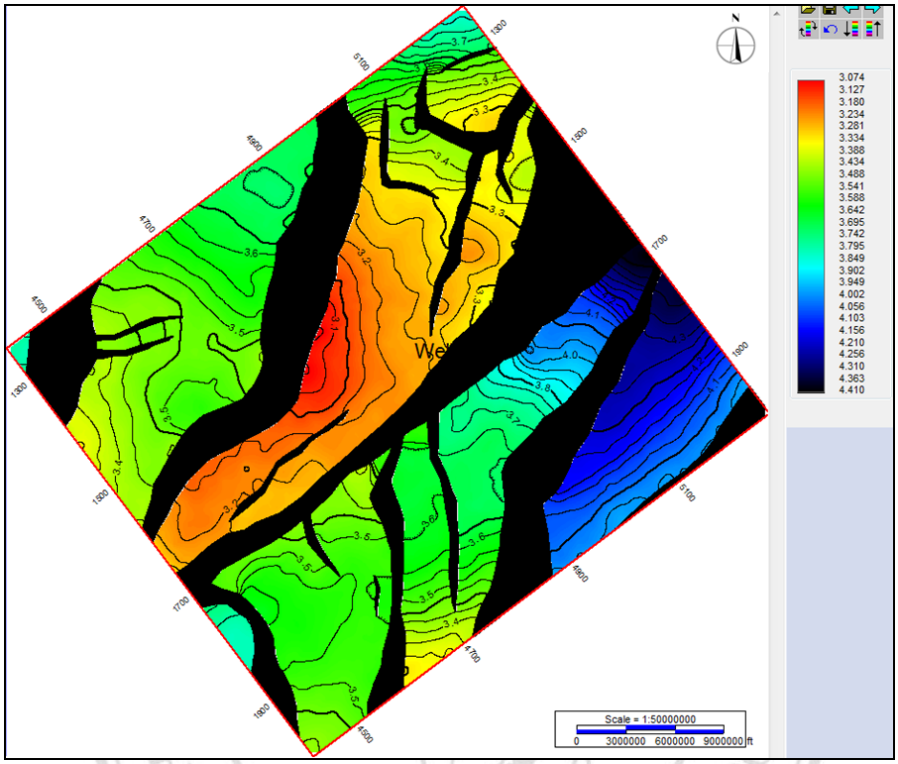

Figure 4.27: Time structure map for horizon T10 (top Oligocene).

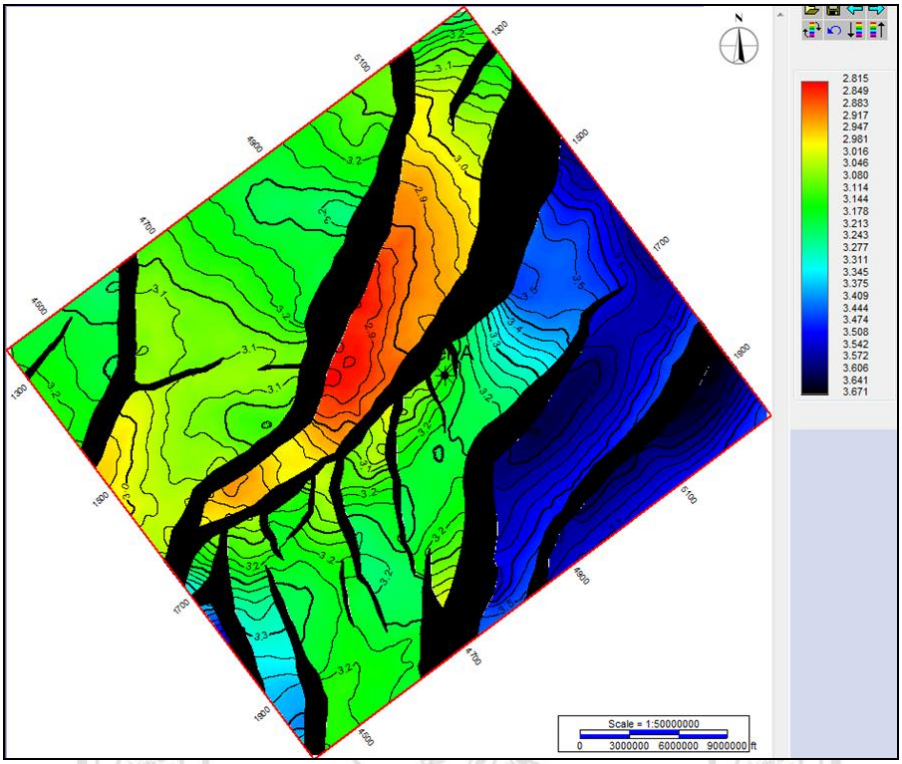

Figure 4.28: Time structure map for horizon T30.

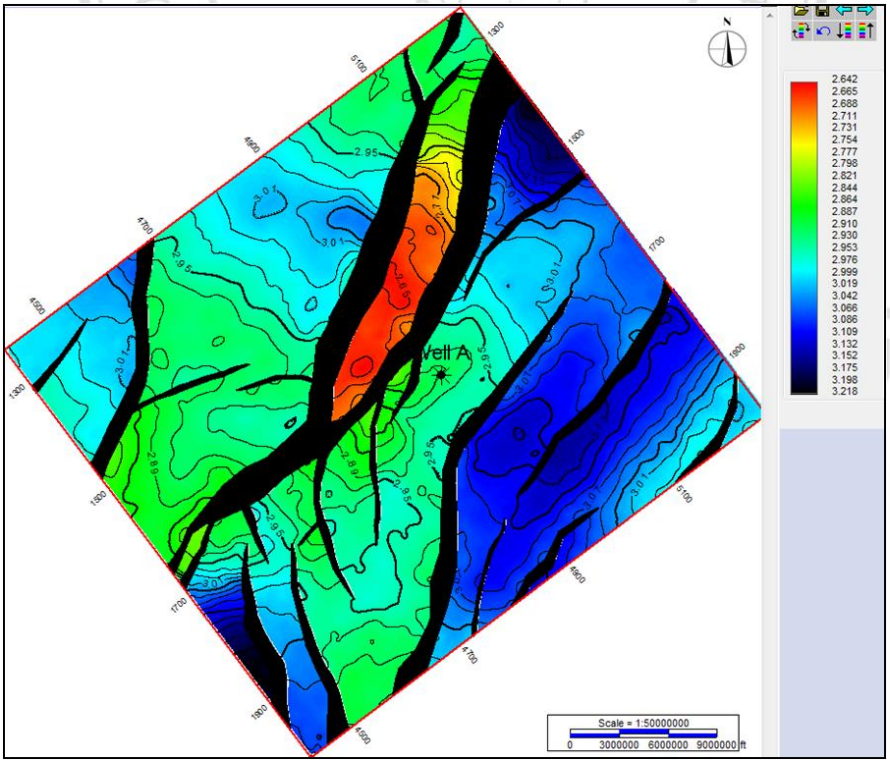

Figure 4.29: Time structure map for horizon Top MMF30.

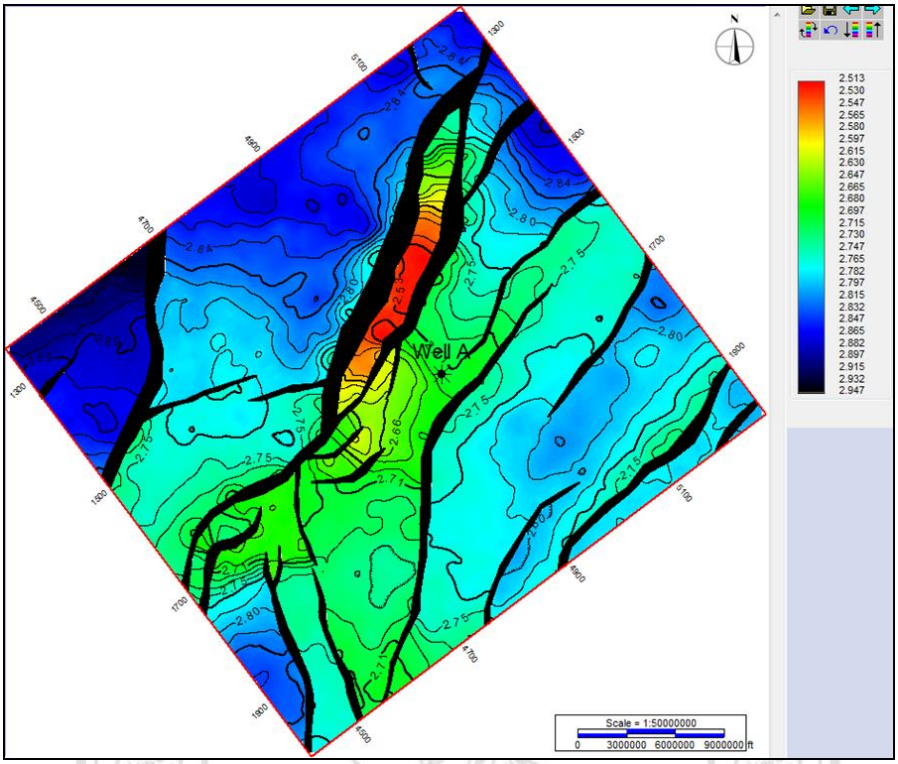

Figure 4.30: Time structure map for horizon T65.

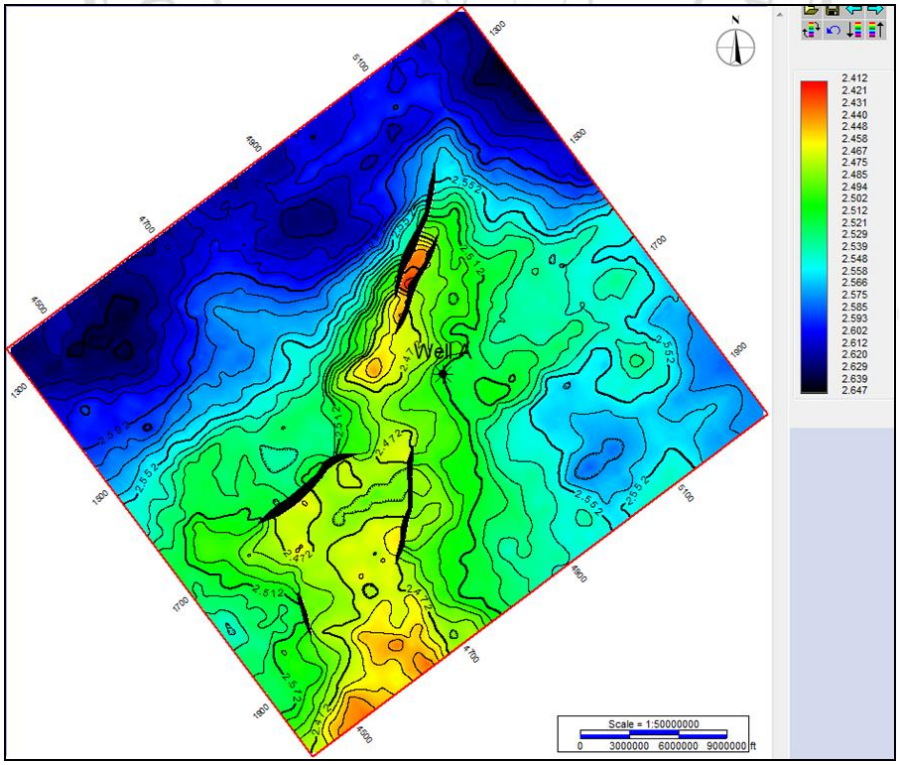

Figure 4.31: Time structure map for horizon Top UMA15.

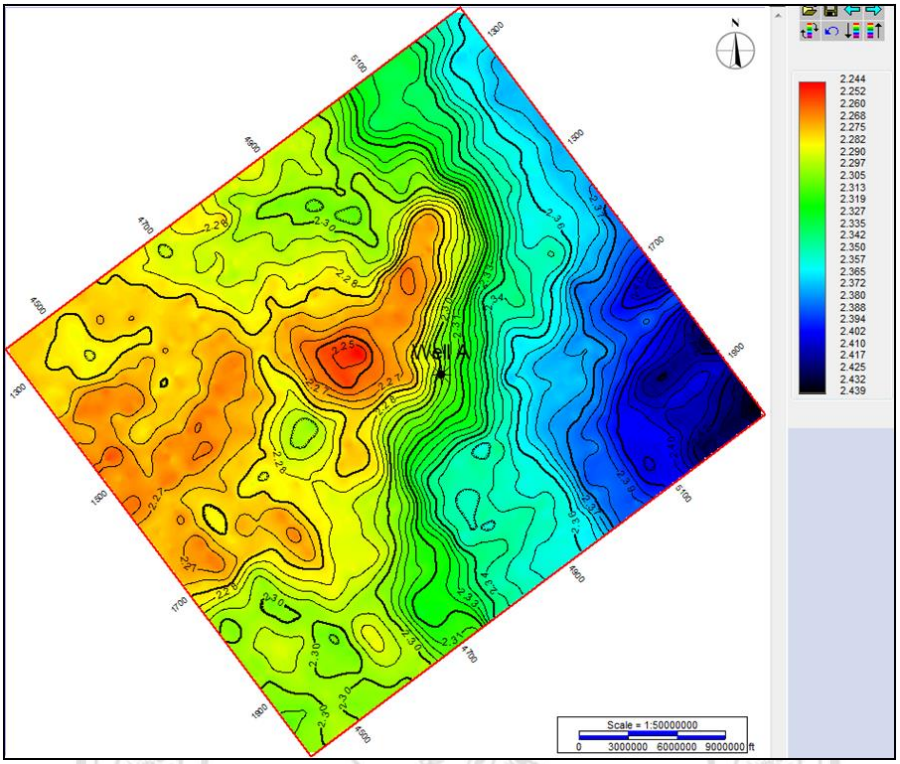

Figure 4.32: Time structure map for horizon T85.

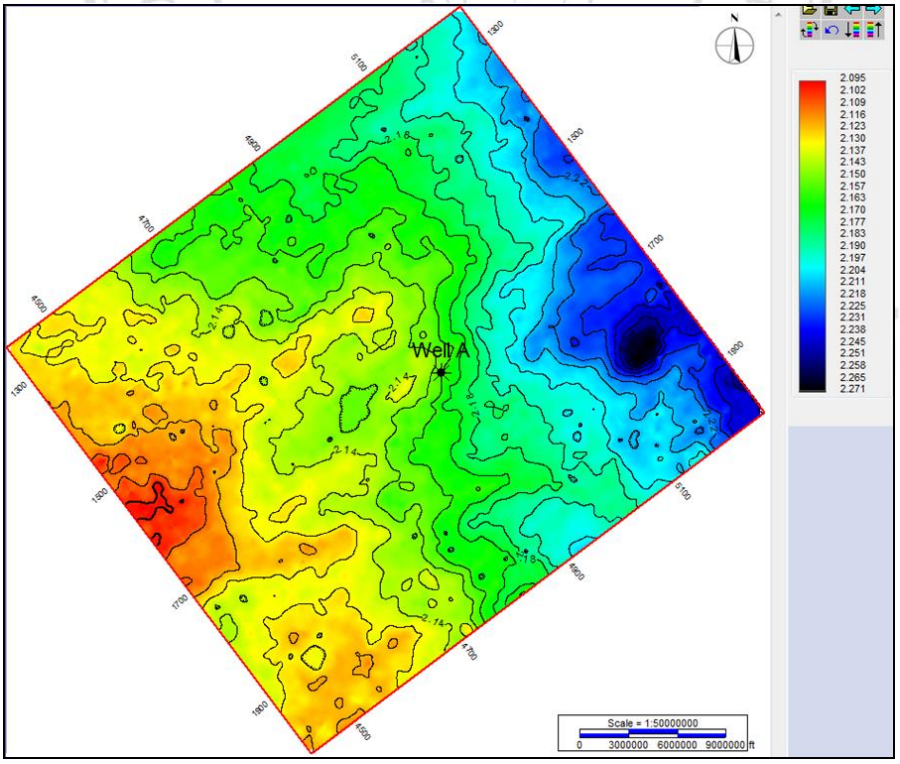

Figure 4.33: Time structure map for horizon T90.